

PHYSICS AT THE ISR  
A REVIEW OF RECENT RESULTS \*)

M. Jacob  
CERN -- Geneva

---

\*) This Review was written after a talk given at the ISR Committee meeting on 21 February 1973, and while the author was visiting NAL.

## 1. - FOREWORD

A short while ago the second anniversary of the first beam-beam collision observed in the CERN intersecting storage rings was celebrated. These two years have witnessed an extremely fruitful activity on this remarkable and unique instrument. The qualities of the beams have continuously increased in perfection. A host of very important results have been collected. They enormously enlarge our knowledge of hadronic processes. It may, of course, seem somewhat frustrating that, extending the range of energy available for experimentation by almost two orders of magnitude, none of the many particles, which could have been protected from human curiosity by high production thresholds only, could yet be found. Quarks, monopoles, intermediate vector mesons, heavy leptons and heavy photons are still challenging so-called possibilities. Discoveries at the ISR did not allow so far for the headlines which such findings would have deserved in a general sense. They, however, made the headlines at recent scientific conferences and in particular at the Oxford Conference last April and at the Chicago-Batavia Conference last September. This is already very much rewarding to all those who pioneered in this new type of research in particle physics. My rôle as a theorist discussing recent results puts me in the privileged but embarrassing position where I can but describe the imposing work of others <sup>1)</sup>. Indeed it would be even unfair to try to present and discuss in a single review the many interesting results which have been collected during these two years of active research. I should accordingly limit this review to what has been learnt during the few months which have elapsed since the Batavia Conference. Detailed reviews already exist for previous periods. The status of research at the ISR was reviewed in great detail at the time of the Oxford Conference <sup>2)</sup> and then at the time of the Batavia Conference <sup>3),4)</sup>, which represent the two 1972 landmarks, respectively, in this domain of physics. I plan therefore here to start from such reviews, minimizing overlap, and to focus on the most recent results. I will therefore discuss in particular the questions of large transverse momentum secondaries, total cross-sections, two-body correlations and finally diffraction phenomena. At the same time, however, I will have to mention only extremely briefly the more matured question of scaling. Evidence for scaling and for a central plateau in the rapidity distribution of secondaries are extremely important steps in our understanding of the high energy phenomena. They should deserve a large fraction of any comprehensive discussion of physics at the ISR. Such questions have, however, already been reviewed rather extensively <sup>2),4)</sup>. Further progress, not already reviewed, would be worth reporting in some detail <sup>5)</sup>. I will, however, be extremely brief on this question here.

We do not have any actual theory to test against experimental results at ISR energy <sup>6)</sup>. We nevertheless expect our present theoretical pictures to be rewarded by some predictive value and it may indeed be said that none of the recent ISR results came as a complete surprise. Picking out two examples, it can be said that theoretical models did allow for a sizeable large transverse momentum component <sup>7)</sup> and for rising cross-sections <sup>8)</sup>. Nevertheless, it should also be said that none of the theoretical ideas which such models embody was matured enough that predictions could be made at a quantitative level or even that the observed qualitative features could be actually predicted against all others so-called possibilities. The actual observation of such effects now provides extremely important pieces of information for the construction of theoretical models of hadron collisions. The actual exploration of such effects raises many questions for which the ISR should be able to give the needed answers. Looking already from the data collected at present, we can easily foresee several years of exciting activity, always hoping, of course, for a more violent surprise.

## 2. - A GLOBAL VIEW OF PROTON-PROTON COLLISIONS AT ISR ENERGY

Proton-proton collisions are mainly inelastic, with  $\sigma_{el}/\sigma_{tot} \sim 0.18$  <sup>3)</sup>. Many particles, mostly pions, are produced with a mean number of  $\pi^-$  of the order of 4 to 5. The transverse momentum distribution of the secondary pions shows the sharp cut-off already found at PS energies, and even more so. The overwhelming majority of pions is produced at low  $p_T$  values, with an exponential distribution  $(d\sigma/dp_T^2) \sim e^{-6p_T} ((\text{GeV}/c)^{-1} \text{ units})$ , empirically valid from  $p_T = 0.2$  to  $p_T = 1 \text{ GeV}/c$  <sup>4)</sup>.

The mean number of pions increases relatively slowly with increasing energy and a logarithmic behaviour is not a bad approximation. The mean number of  $\pi^-$  produced in pp collisions varies from 0.6 to 4 only between 10 and 1000 GeV incident energy. Other secondaries such as  $K^-$ , and even more so  $\bar{p}$ , show a very rapid rise between PS and ISR energies and then a much slower increase with energy. Between 20 and 1000 GeV the mean number of  $\bar{p}$  produced per collision rises from  $2 \times 10^{-3}$  to 0.2. It is, however, already 0.07 at 200 GeV. The  $p_T$  distributions are wider for K, and even slightly more so for  $\bar{p}$ , than they are for  $\pi$  <sup>9)</sup>.

Focusing first on low transverse momentum secondaries ( $p_T < 1 \text{ GeV}/c$ ), which represent the overwhelming majority, scaling appears as the prominent property <sup>2),4)</sup>. Scaling can be abstracted from different theoretical pictures <sup>10)</sup>, as a very general property of inclusive distributions. It implies that invariant distributions, corresponding to specific types of secondaries  $i$ , namely  $f^i = E(dN^i/dp_T^2 dp_L)$ , at fixed  $p_T$  and  $x = (2p_L/\sqrt{s})$ , should become eventually independent of energy at large enough energy. We have denoted by  $p_T$ ,  $E$  and  $p_L$ , the transverse momentum, the energy and the longitudinal momentum of the observed particle, respectively. As usual  $\sqrt{s}$  is the centre-of-mass energy and  $x$  is referred to as the Feynman scaling variable. In other words, the inclusive distribution should asymptotically depend on  $p_T$  and on the longitudinal centre-of-mass momentum  $p_L$  scaled according to the centre-of-mass energy, but not on  $\sqrt{s}$ .

The first results obtained at the ISR, mainly involved particle survey <sup>2)</sup>. They provided remarkable evidence for such a scaling property <sup>2),4)</sup> thus tested on a very wide energy scale. With the amount of information now available <sup>2),4),5)</sup>, a clear hierarchy in scaling property emerges.

It is convenient to define three types of secondary particles, even though any clear distinction is impossible except in very specific regions of phase space. The first type corresponds to fragments of the incident particles. They are secondaries which are produced with rapidities <sup>11)</sup> which are similar to those of the incident particles (within 2 units, say) <sup>12)</sup>. Such particles are relatively slow when considered in the rest frame of one of the incident particles. In terms of  $x$ , one may consider pions with  $0.6 < |x| < 0.1$  as proton fragments, though such a choice is, of course, not binding in terms of the actual dynamics of the reaction. At PS energy, with a total rapidity interval of 4 units, it is difficult to point out something which is clearly not in the fragmentation region. However, as the centre-of-mass energy increases, the total rapidity interval increases as  $\ln s$  to reach typically 8 units at ISR energies. One may then point out a central region where secondaries are several units away in rapidity from any of the two incident particles. This is also referred to as the pionization region. In terms of  $x$ , it corresponds to the neighbourhood of  $x = 0$ . This is, however, where phase space is the widest for each secondary and, indeed, where most of the multiplicity is found at ISR energies.

Finally it is convenient to consider separately final particles which can be almost unambiguously associated with one of the primary particles after quasi-elastic scattering off the other one. At ISR energy this corresponds to very high energy protons with  $1 < x < 0.95$ .

Such a classification turns out to be convenient but does not correspond yet to any precise separation between production mechanisms. As is now well known, a hierarchy pattern in scaling behaviour holds. Pion distributions already practically scale at PS energy in the fragmentation region. They still rise, however, by a factor of about 2 at  $x \approx 0$  between PS and ISR energies, but reach - to a 10% approximation - a limiting behaviour throughout the ISR energy range <sup>13)</sup>. As expected from proton fragments, the scaling limits met in the fragmentation region are higher for  $\pi^+$  than they are for  $\pi^-$ . The behaviour at  $x = 0$  approaches, however, a common limit with increasing energy. Distributions for other secondaries show very similar trends. Nevertheless the approach to a limiting behaviour is the slowest the highest the reaction threshold is and, accordingly, the lower the corresponding multiplicity is. If the  $\bar{p}$  distribution in the fragmentation region reaches practically its limit at ISR energy, the observed rate is much higher than that measured at PS energy. At the same time the  $\bar{p}$  distribution at  $x \approx 0$  still rises significantly throughout the ISR energy range. In this review I will not dwell on these questions and only contrast the behaviour of the  $\pi^+$  and  $\pi^-$  distributions, on the one hand, to that of the  $p$  and  $\bar{p}$  distributions on the other hand, all considered at  $x = 0$  for fixed  $p_T$ . Figure 1a shows the  $\pi^+$  and  $\pi^-$  inclusive distributions at  $x = 0$  different  $p_T$  values, as measured by the Saclay-Strasbourg collaboration. For pions one clearly sees the approach to a common limiting behaviour (within errors) whereas central distributions at PS energy are definitely lower and different from each other. For  $\bar{p}$  a sustained rise still exists throughout the ISR range when the proton distribution shows the competitive effects attached to the leading particle effect and to the formation of  $p\bar{p}$  pairs respectively. This is seen in Fig. 1b. One is still far from any expected asymptotic behaviour. The same results have been independently obtained by the British-Scandinavian collaboration which can probe an appreciable rapidity interval around  $y = 0$  whereas the Saclay-Strasbourg data presented here are limited to production at  $90^\circ$ . One should of course mention that the existence of a finite limiting value for the pion distribution is associated with the presence of an extending rapidity plateau when the inclusive distribution is presented in terms of rapidity. Observation of such a phenomenon constitutes an important discovery. The detailed results of the British-Scandinavian collaboration have, however, already been reviewed <sup>2),4)</sup>.

Such a brief discussion of scaling properties should not be understood as undetermining the importance of such results. Much to the contrary, they represent an extremely important step in our understanding of hadronic phenomena. It should further be stressed that ISR results not only provide evidence for a scaling limit <sup>13)</sup>, but also information about the actual approach to this limit, which for particular secondaries is far from being reached at 2000 GeV. Indeed, if scaling is extremely important, verifying it over and over again may eventually become dull. Studying with more precision the approach to scaling remains extremely interesting. The purpose of this review is, however, to focus on those results which were not already much discussed at the Batavia Conference and to which we now turn.

### 3. - LARGE TRANSVERSE MOMENTUM PHENOMENA

The overwhelming majority of secondaries is produced at relatively low transverse momentum ( $p_T < 1$  GeV/c) and, as already mentioned, an exponential behaviour, with a slope of  $6 \text{ GeV}^{-1}$  gives a fair fit to the  $p_T$  dependence of the pion yield. It was therefore tempting to search for special features at large values of  $p_T$ , beyond the crowd of "commonly" produced hadrons, in order to probe for yet unknown manifestations of electromagnetic or weak interactions. This turned out to be a disappointment. What is found instead is that the pion yield at large  $p_T$  ( $p_T > 2$  GeV/c, say) is much larger than expected from the simple extrapolation of the exponential behaviour met for  $p_T < 1$  GeV/c. This is of course also extremely interesting. The importance of this effect is clearly seen in Fig. 2a, which gives data on  $\pi^0$  obtained by the CERN-Columbia-Rockefeller collaboration at  $\sqrt{s} = 53$  GeV <sup>3),4),14)</sup>. It is also seen in Fig. 2b which groups together data on charged pions <sup>15)</sup> at two different energies obtained by the Saclay-Strasbourg collaboration <sup>5),16),17)</sup>. The observed yield is much above what the naive extrapolation of low  $p_T$  data would suggest. The observation of such a phenomenon did not come as a complete surprise. It had been emphasized previously that, in view of the results obtained at SLAC on deep inelastic electron scattering, production of pions at large transverse momenta should eventually show a much weaker  $p_T$  dependence (inverse power, say) than what observed at  $p_T < 1$  GeV/c, thus giving much larger yields than what could be expected from an exponential dependence <sup>7)</sup>. Lower bounds could even be calculated from electromagnetic interaction alone. This led to predict that, at least for  $p_T < 5$  GeV/c, the exponential behaviour

found at small  $p_T$ , should no longer hold. What is seen in Fig. 2 is a departure from the initial exponential behaviour which is already very pronounced at  $p_T = 3 \text{ GeV}/c$  ! We are therefore facing an effect which, if estimated in terms of strength functions, similar to those defined in deep inelastic scattering, should be labelled as a strong interaction process. It is scaled up by  $10^4$  as compared to what one can calculate for an electromagnetic interaction. At present this provides too strong a background to measure with any confidence an actual electron component <sup>17)</sup>. This may be considered as a set-back for the original search for new electromagnetic or weak effects. Evidence for such new hadronic phenomena represents, however, an important discovery. Its study should be very informative about the proton structure at extremely small distances. Furthermore, as shown by the observed rates, the ISR appears as an excellent instrument to study it.

At present we are at the first exploratory steps and we have only somewhat fragmentary information. Important features can, however, already be ascertained. If the low  $p_T$  distribution scales at ISR energies, this appears no longer to be the case beyond  $3 \text{ GeV}/c$ . This is seen in Fig. 2b. Figure 3 gives the integrated rate for  $3.2 < p_T < 5.2 \text{ GeV}/c$  measured in the Saclay-Strasbourg experiment (differential cross-section at  $90^\circ$ ). It practically increases linearly with  $s$ . It should be stressed, however, that production thresholds for such final states are relatively large and that scaling, if also holding eventually, could be belated even more so than for  $\bar{p}$  production.

Contrasting with the charge symmetry of the low  $p_T$  component (Fig. 1a), inclusive distribution at large  $p_T$  shows a strong charge effect. Figure 4 gives for instance the yields at fixed  $p_T$ , observed for positive and negative particle respectively, by the Saclay-Strasbourg collaboration at  $x = 0$ . The experiment covers the ISR energy range and one sees a lack of (or belated) scaling appearing with increasing  $p_T$ . The positives are clearly more abundant than the negatives at large  $p_T$ , with a ratio of the order of 1.3. This result has independently been obtained by the British-Scandinavian collaboration <sup>5)</sup>. This excess of positives is to be associated with a modification of the relative yields of pion and heavier particles as  $p_T$  increases. At low  $p_T$  ( $p_T < 1 \text{ GeV}/c$ ) one observed mainly pions and practically as many negative as positive ones. As  $p_T$  increases ( $p_T > 3 \text{ GeV}/c$ ), the pion component could not even keep a leading rôle. This is suggested by the results shown in Fig. 5 which displays the power and limitation of present

spectrometers. At low  $p_T$  ( $p_T < 1$  GeV/c), particles are sorted out by time of flight measurements and pions predominate <sup>2),4)</sup>. At large  $p_T$  ( $p_T > 3$  GeV/c) pions can be separated out by a Cerenkov trigger. At intermediate momentum  $1 < p_T < 3$  GeV/c, only the distribution of positives (negatives) can be obtained. The results of the Saclay-Strasbourg experiment shown in Fig. 5 should be soon improved upon by new results from the British-Scandinavian collaboration. At present extrapolating naïvely the positive yield beyond 3 GeV/c and the pion yield below 3 GeV/c one finds an embarrassing mismatch. It seems that at 3 GeV/c the global positive yield could be several times the pion yield. The preliminary results of the British-Scandinavian collaboration would, however, not indicate that it is that much, but rather give at most equal weight to the heavy and pion component, respectively. This a very challenging question. It seems in any case that at large  $p_T$  ( $p_T \sim 3$  GeV/c, say) the pions have left the overwhelming supremacy which they show over all other secondaries at low  $p_T$ . The Saclay-Strasbourg and British-Scandinavian results on total positive (negative) are in good agreement ( $p_T < 3$  GeV/c) and show little deviation from scaling with at most a slow rise (Fig. 4). This should be compared with the behaviour of the  $\pi^0$  component <sup>4),14)</sup> at similar  $p_T$  and also with the behaviour of the pion component at larger  $p_T$  <sup>5)</sup>.

At present one may look at these results from different theoretical view-points and the different over-all pictures which they suggest are extremely useful at phrasing the questions to be asked now. There is one common feature though in most theoretical pictures so far proposed and it is that there is some point-like coupling from which a factorizable inverse power  $(p_T^2)^{-n}$  behaviour eventually follows. It shows up at large enough  $p_T$  over that associated with standard "soft" hadronic mechanisms giving typically Gaussian behaviours. How this is embedded in the reaction amplitude as a whole distinguishes, however, various schools of thought. This common approach, centred on a point-like coupling, has been particularly emphasized by Landshoff and Polkinghorne <sup>18)</sup>. Constructing the full amplitude one may, however, emphasize the over-all multiperipheral character of the collision, as recently done by Amati, Caneschi and Testa <sup>19)</sup>, or its parton aspect, as already described by Berman, Bjorken and Kogut <sup>7),20)</sup>. In the first case, one may hardly consider a small and a large transverse momentum component. There is a smooth transition across the whole  $p_T$  range. In the second case, one is led to distinguish more clearly hard parton collisions, giving large  $p_T$  secondaries, from a dominant production mechanism with low  $p_T$  secondaries. Inclusive data, which average over all collisions, are at present not sufficient enough to decide even between two such extreme pictures. Simple correlations should already be extremely helpful, as discussed next.

The two extreme pictures, which one may thus consider following either a multiperipheral or a parton prejudice, are graphically depicted in Fig. 6. Figure 6a is an over-all multiperipheral amplitude where one of the central particles (i) happens to have a large transverse momentum, an unlikely but possible configuration. Constructing a multiperipheral amplitude, one tries to minimize transverse momenta along the multi-exchange chain. There is obviously a strong limitation on what can be done when a particular secondary is produced with large  $p_T$ . However, this being done, configurations where another secondary produced nearby along the multiperipheral chain (similar rapidity) and with an opposite value of  $p_T$  should be highly enhanced, as opposed to others where a large momentum transfer is to be found in several consecutive steps along the chain. This results in two prominent qualitative features. Firstly, if a secondary with a large transverse momentum is observed, one should expect that another secondary, with similar rapidity, is balancing this particularly large transverse momentum. One also expects a local balancing of quantum numbers and therefore a large transverse momentum proton calls for a large transverse momentum anti-proton in the opposite direction. Secondly,  $p_T$  and quantum numbers being properly balanced, relatively large rapidity gaps should be found on either sides of these two secondaries (Fig. 6b) in order to minimize the momentum transfer along the chain, once a system with an invariant mass of the order of  $p_T$  is produced. These gaps should increase as  $\ln p_T$ . One therefore expects a decrease of the multiplicity at rapidity values similar to those of the observed secondary and little change from what observed in most collisions when considering rapidities much different from those of the observed central secondary with large  $p_T$ . The dominant amplitude is shown in Fig. 6a. One far off-shell particle is exchanged between two secondaries with large and roughly opposite transverse momenta and two almost on-shell two-body (multiperipheral) amplitudes are included on either sides. The propagator imposes a factor  $(p_T^2)^{-2}$  in the inclusive distribution<sup>21)</sup>. The remaining part of the amplitude is calculated using leading Regge behaviour. At large  $p_T$  and  $\sqrt{s}$  it can then be written as a power of  $p_T$  times a function of  $p_T/\sqrt{s}$  and of course of  $y$ , the rapidity of the observed secondary. One thus writes<sup>17)</sup>

$$f(p_T, y) \sim \left(\frac{1}{p_T^2}\right)^n F\left(\frac{p_T}{\sqrt{s}}, y\right) \quad (1)$$

The exponent  $n$  is left as a free parameter since its actual value depends on the spins of the relevant particles<sup>22)</sup>. The function  $F$  reaches a limiting value at infinite energy. Hence the inclusive distribution scales for arbitrary large  $p_T$  provided that  $s$  is large enough and the more so as  $p_T$  increases. The approach to scaling may also depend on  $y$ <sup>23)</sup>. Observation of such an effect outside the wide angle region would be very interesting. As far as one may know at present, there is not any strong angular dependence.

Following now a parton picture, the large value of  $p_T$  results from a primary hard parton encounter with wide angle scattering, which is not negligible for partons. One therefore expects a factorizable inverse power behaviour, namely  $(p_T^2)^{-2}$ . One also has to calculate the inclusive distribution attached to the showers of secondaries associated with the scattered parton. At large  $p_T$  and  $\sqrt{s}$  it also depends on a scaled variable  $p_T/\sqrt{s}$  together with the rapidity  $y$  of the observed particle, only. This was worked out in detail by Berman, Bjorken and Kogut<sup>5)</sup>. Summarizing in both approaches one expects that, once an inverse power of  $p_T$  is factored out, the inclusive distribution should depend on  $y$  and  $p_T/\sqrt{s}$  only, with an asymptotic scaling for each  $p_T$ .

The parton picture<sup>24)</sup> can be used to make more specific qualitative predictions. The key point is that the two hard partons, once scattered at wide angle, have very little overlap in phase space with the other parton constituents. They are therefore expected to decay into partons which share the momentum of the initial one unevenly. This gives hard and wee partons, all roughly in the direction defined by the initial scattering (small transverse momentum in the decay chain). The wee ones only interact strongly with other partons with an over-all balancing of quantum numbers as required by conservation laws. The harder ones, however, which are far away from them in phase space, should not. This is represented graphically in Fig. 6d. We now make the assumption, which is at the core of the parton model, that the final actual hadronic state has much overlap in phase space with the final parton state thus obtained through parton scattering and decay. We are then led to expect two jets of secondaries spread in momentum but relatively well collimated in opposite directions. The larger the momentum of the initially scattered parton, the larger the momentum of the hardest actual secondary should be. The larger also should be the over-all multiplicity in the jet or, for wide angle secondaries, the associated multiplicity at similar rapidity. The hardest secondary should also show a definite

memory of the quantum numbers of the initially scattered partons. Since there are more positive than negative ones, a definite positive excess should result and, more generally, one should expect an excess of particles over antiparticles. A large  $p_T$  proton does not call for a large  $p_T$  antiproton in the opposite direction. This is to be contrasted to the particle-antiparticle symmetry which one should expect in a multiperipheral picture up, of course, to non-asymptotic terms. More striking is the associated multiplicity increase at similar rapidities which can be contrasted to the multiplicity decrease expected in a multiperipheral picture \*).

In both extreme pictures one is led to expect the pion supremacy, enforced at low  $p_T$ , to gradually disappear with increasing  $p_T$ . In a multiperipheral picture what matters is  $m_T = (p_T^2 + m^2)^{\frac{1}{2}}$  rather than  $p_T$  and, for large enough  $p_T$ , all masses are kinematically on the same footing. For instance, kaon should not be discriminated against pions any longer when  $p_T$  is large enough. One would then expect as many  $K^-$  as  $K^+$ . In a parton picture, the particles in each jet should share the available energy unevenly. In any simple model the heavy particles get larger momenta than the light ones. If one insists on observing a particle at large  $p_T$ , he biases himself in favour of a heavy secondary even though pions might strongly dominate in the jet. The charge effects already discussed (Fig. 5) could favour a parton picture. Even more relevant in that respect is the increase of the associated multiplicity with  $p_T$ , recently reported by the Pisa-Stony Brook collaboration and by the CERN-Columbia-Rockefeller collaboration <sup>25)</sup>. Data are still preliminary and should not be discussed at great length here. The Pisa-Stony Brook group sees an increase of the charge multiplicity at wide angle when the transverse momentum of a required wide angle  $\gamma$  ray is increased. At the same time the multiplicity at small angle (very fast secondaries) drops. The forward-backward asymmetry of the central multiplicity, defined with respect to the direction of the  $\gamma$  ray, increases but remains small. The CERN-Columbia-Rockefeller group finds that the charged multiplicity at  $90^\circ$  highly increases when requiring a  $3 \text{ GeV}/c$   $\pi^0$  from what measured on the average. This is not only found in the direction opposite to the  $\pi^0$  (factor 2.5, say) but also in the direction of the  $\pi^0$  (factor 1.8, say). At the same time one also finds a strong positive "back to back" correlation between large transverse momentum  $\pi^0$ 's. The large transverse momentum particles are not isolated. Events where they show up have rather large multiplicities associated with them and may show a two-jet structure, a point worth exploring in detail.

---

\*) As is well known, once the information is available, both pictures may be adjusted enough so as to meet the results. They are useful anyway at phrasing such questions.

It should be stressed, of course, that the cross-sections associated with such configurations are relatively small. Nevertheless we may well see in this particular way a new type of hadronic phenomena in direct relation with the scaling behaviour of strength functions observed at SLAC. Exploration of such processes is just beginning. The yields are such that they can be thoroughly studied at ISR. Results from the CERN-Munich streamer chamber, the Saclay-Strasbourg double spectrometer (later associated to the CERN-Columbia-Rockefeller lead glass detectors) and the British-Scandinavian collaboration, should be available in the near future. This should resolve the present puzzle of the mean constitution of the large transverse momentum component and provide many new data on correlations and associated multiplicity results which, as already emphasized, are extremely useful. Later on the split field magnet facility and, maybe, calorimeter studies, should permit pushing this analysis much further in detail.

#### 4. - THE RISING TOTAL CROSS-SECTIONS

It is very difficult to measure total cross-sections at the ISR. It is not the purpose of this review to emphasize that but rather to comment on the results presented in two recent preprints <sup>26),27)</sup> by the CERN-Rome and the Pisa-Stony Brook collaborations, respectively <sup>28)</sup>. The first group uses the optical theorem and actually measures  $dN/dt$ . Normalization to the Coulomb peak is even possible for the lowest two energy points. The second group measures directly the number of collisions, being sensitive to almost all possible configurations of secondaries. The reported results are shown in Fig. 7a. They demonstrate that total cross-sections at ISR energy are significantly higher than at Serpukhov energy and indicate a definite rising trend.

That the total cross-section rises is again not a complete surprise. The limited range of strong interactions allows for a logarithmic rise. Limits set by the Froissart bound and later developments <sup>8)</sup> are indeed much above what is observed.  $\ln s$  increases by a factor 2 across the ISR energy range. Figure 7a shows, for instance, a casual fit obtained with a  $\ln^2 s$  term. What should be noticed in any case is that the effect is too big to be blamed on long-range electromagnetic effects. Semi-classical analogies and search for J plane simplicity did, however, favour for a long time finite limiting

values for total cross-sections. This may still be a valid point and this is illustrated by the other casual fit of the  $\sigma (1 - B(\log s + c)^{-1})$  type also given in Fig. 7a. This is inspired by the Gribov-Reggeon calculus<sup>8)</sup>, which associates, to an eventually dominant Regge pole, logarithmically decreasing Regge cut corrections. A finite limiting behaviour exists but it is only slowly approached from below. What the fit given in Fig. 7a shows is that the ISR energy range would then still correspond to a transition domain where the cross-section is far below its asymptotic limit of 60 mb or so. In such a case exchange degeneracy would be strongly violated in the pp case, with a strong Regge contribution conspiring at producing an almost constant cross-section at present machine energy<sup>29)</sup>.

One may obviously not conclude straightway when the question of cross-sections rising indefinitely, as opposed to cross-sections rising to a moderate limiting value, is the challenging question. This makes it the more so interesting to study  $\bar{p}p$  and  $K^+p$  total cross-sections at NAL energies. The  $K^+p$  cross-section, with exchange degeneracy as a stronger constraint, rises first and may already show a definite inflection not seen now with pp cross-sections, the accuracy of which can hardly be increased.

A rising cross-section implies through dispersion relations a positive real part of the forward elastic amplitude. The ratio of the real to the imaginary part, negative at present machine energy, should vanish, as it is indeed found to do in the CERN-Rome experiment<sup>26)</sup>, becomes positive, passes through an extremely broad maximum and then eventually goes to zero. A recent calculation<sup>30)</sup> shows a maximum of the order of 0.1 practically reached at top ISR energy or 2000 GeV. The corresponding fit to the total cross-section uses an eventually leading  $\ln^2 s$  term with a coefficient of 0.53 mb. This is a small value as compared with available bounds<sup>31)</sup>. It should then be attributed to a short-range effect. A logarithmic approach to an asymptotic limit yields a similar general behaviour for the ratio of the real to imaginary part.

What may be worrisome, though, with total cross-sections rising as fast as  $\ln^2 s$ , is the observed behaviour of the slope parameter of the elastic differential cross-section at small  $|t|$ . As measured by the Aachen-CERN-Genova-Harvard-Torino collaboration, it definitely rises between PS energy and ISR energy (from 10 to 12.5, say), but its derivative as a function of  $\ln s$  does seem to decrease with increasing energy<sup>3)</sup>. There is definitely shrinking of the diffraction peak but the rate of shrinking could decrease with energy. It is, however, a consequence of s channel unitarity (and simplicity) that if the total cross-section grows indefinitely the slope of

the diffraction peak has to grow <sup>32)</sup>. More precision on ISR data would help. Results from NAL, soon available, should also indicate which is the actual trend. While briefly commenting on elastic scattering, one should mention the clear dip at  $|t| = 1.2 \text{ (GeV/c)}^2$  reported by the Aachen-CERN-Genova-Harvard-Torino collaboration, which stands for a neat diffraction minimum. This was already reported at Batavia <sup>3)</sup> and, though a very important point, will not be further discussed here. Figure 7c summarizes available data on the slope parameter.

In conclusion, we have, with rising cross-sections, a new and extremely important fact. Its interpretation in our present theoretical framework cannot be considered alone. With more information about the behaviour of the real part and of the slope parameter, but - even more so - with a detailed comparative study of total cross-sections and elastic scattering in other channels, as possible at NAL, a comprehensive picture should emerge. As shown by the casual fits of Fig. 7, it is too easy to meet the reported rise without having to meet at the same time many other pieces of data.

## 5. - TWO-PARTICLE CORRELATIONS

Scaling, which was briefly reviewed, appears as so general a property that much different pictures of particle production have it as a common property. Indeed, it involves only particle yields averaged over all possible configurations and it is hard to infer any specific detail of the production mechanisms from the existence of a scaling limit only. At the same time, the mean number of particles is so high that we could, at present, hardly handle a complete description of each inelastic collision, were it available. We could for a while be simply swamped by the amount of information. It will in any case take some time before such a detailed analysis can actually be done for average and high multiplicity reactions.

As an intermediate step, one may, however, already obtain and analyze some data about correlations between secondary particles or, more generally speaking, about the variation of any particular yield with the parameters (quantum numbers and momentum) defining an observed secondary particle. A momentum correlation between two secondaries involves already six variables  $(p_{L1}, p_{L2}, p_{T1}, p_{T2}, \varphi_{12}, \sqrt{s})$ , where  $\varphi_{12}$  is the angle

between  $p_{T1}$  and  $p_{T2}$ . Even when limiting ourselves first to such correlations, there are many different double distributions which can be obtained, selecting a particular set of variables and fixing the others or averaging over them. Presenting even the most salient feature of the data already available in any comprehensive way would involve much more than this review can accommodate <sup>25),33)</sup>. Only one particular facet of correlations will be discussed here, namely rapidity correlations among two wide angle secondaries, averaging over transverse momentum distributions. This involves therefore essentially correlation among pions (charged pions for correlations among charged particles, charged and neutral pions for correlations among one charged particle and a  $\gamma$  ray...). This choice is motivated by the large amount of information already collected. It should be stressed though that many interesting pieces of data about other types of correlations are quickly becoming available <sup>25)</sup>. Limiting anyway ourselves to this type of analysis, we may compare double differential distributions  $d^2\sigma^{ij}/dy_1 dy_2$  to the corresponding single particle distributions  $d\sigma^i/dy$  and  $d\sigma^j/dy$ . Using rapidity  $y$  instead of longitudinal momentum  $p_L$  is quite natural when focusing on wide angle secondaries <sup>11)</sup>. Indeed for all experimental results here considered one has to use  $\eta$  instead of  $y$ .

Correlations are expected on very general grounds and should take different aspects whether the two secondaries are in a similar region of phase space or not <sup>34)</sup>. In terms of rapidity, one is thus led to distinguish between long-range and short-range correlations <sup>35)</sup>. A long-range effect involves the available rapidity range as a whole  $Y$ . On the contrary a short-range effect involves only a fixed rapidity interval which should eventually become much smaller than  $Y$  with increasing energy. Resonance formation or, more generally speaking, clustering effects among secondaries result in positive short-range correlations. In the Mueller approach <sup>36)</sup> Pomeron exchange in the pertinent discontinuity of the eight-point function will give no correlation at large  $\Delta y$  <sup>37)</sup>. For finite rapidity differences, still sizeable secondary Regge trajectory contributions result in correlations. Nevertheless, they are expected to vanish with rapidity difference  $\Delta y$  as  $e^{-(\alpha_p - \alpha_R)\Delta y}$ , where  $\alpha_p$  and  $\alpha_R$  stand for the intercept of the Pomeron and leading secondary Regge trajectory, respectively. Again one finds short range effects with a rapidity range (exponential decrease) of two units  $L = (\alpha_p - \alpha_R)^{-1}$ . The correlation effect spread over four units of rapidity only <sup>38)</sup>. Such an exponential behaviour holds of course only if  $\Delta y$  is large enough. Not up to  $\Delta y = 0$  !

We may also phrase the distinction between short and long-range correlations in a different way, asking what type of information is gained through the observation of one secondary at rapidity  $y$ . This may give information about the collision process as a whole and in particular the multiplicity of the event. It will then provide information about the possible occurrence of another secondary particle at any available rapidity. This is a long-range effect. On the contrary it may practically provide only information about the probability of finding another secondary particle in a similar region of phase space or nearby in rapidity. This is then a short-range effect.

Evidence for the two effects at ISR energies is illustrated by Figs. 8a and 8b. Both figures correspond to results of the Pisa-Stona Brook collaboration. In Fig. 8a <sup>4)</sup>, one has rapidity distributions attached to different charged multiplicities. They are clearly different, being more peaked at lower centre-of-mass rapidity for higher values of charge multiplicity <sup>39)</sup>. Observing a particle at any given rapidity biases one towards certain multiplicities and hence towards some more likely rapidity distributions for any other particle to be observed. This implies clearly long-range correlations. Such an effect is particularly strong for relatively large rapidities where the different semi-inclusive distributions differ most. At low rapidity, however, the observation of a secondary does not distinguish much (probability wise) between multiplicities ranging over a comfortable set of values. Short-range effects may therefore show up more clearly by themselves and this is what is seen in Fig. 8b. The two-particle rapidity distributions reach their respective maximum when  $y_1 = y_2$  and this independently of  $y_1$  in the whole range which is covered. This is an obvious short-range effect, namely, the observation of a particle favours the observation of a second one at the same rapidity. One should notice, however, that the shape of the two-particle distribution changes gradually with  $y_1$ . The observed correlation does not depend on  $\Delta y$  only (short-range effects alone). There is also a  $y_1$  dependence (long-range effect also).

In order to analyze such correlation effects one may use the actual value of these correlations now measured as a function of rapidity and energy. The tricky interplay between definite long-range effects and definite short-range effects is such that one should urge experimentalists to give at least separately  $d\mathcal{N}^{ij}/dy_1 dy_2$ ,  $d\mathcal{N}^i/dy$  and  $d\mathcal{N}^j/dy$  and to avoid the

temptation of summarizing the observed effect through a single correlation function. Dividing both distributions by  $\sigma_{inel}$  one usually defines next rapidity densities for inelastic events <sup>40)</sup> and may "measure" the correlation through

$$R^{ij}(y_1, y_2) = \sigma_{inel} \frac{d^2\sigma^{ij}}{dy_1 dy_2} \left( \frac{d\sigma^i}{dy_1} \frac{d\sigma^j}{dy_2} \right)^{-1} - 1 \quad (2)$$

As seen from the data given in Fig. 8b, this ratio takes its highest value when  $y_1 = y_2 = 0$  and for each  $y_1$  (not too large) when  $y_1 = y_2$ . This indicates positive short-range correlations or that the secondaries produced at wide angle have a tendency to cluster in rapidity (or phase space) more than one could casually conclude from single-particle distributions which only provide an average rapidity density  $\ell = (1/\sigma_{inel})/(d\sigma/dy)$ .

We may then visualize a typical rapidity configuration as drawn in Fig. 9a. We represent a rapidity distribution with some clustering among proton fragments on either ends <sup>41)</sup> but also among low rapidity (wide angle) particles which we intentionally separate from clear fragments <sup>42)</sup>. Increasing the energy, the available rapidity interval increases. Two extreme possibilities are then offered in Figs. 9b and 9c, respectively. With more energy available, larger clusters of particles could be formed (Fig. 9b). The multiplicity would increase but, together with it, the density in rapidity found in many configurations. Two-particle correlations at wide angle would then increase with energy. Following the other extreme, (Fig. 9c), the cluster size is kept the same but more clusters can be formed in each event. Produced particles are spread over the available rapidity interval and local density fluctuations, associated with each cluster, are then independent of energy. Furthermore,  $R(y_1, y_2)$  should be independent of  $y_1$  for low enough values of  $y_1$  ( $y_2$ ) as the local density distribution in rapidity should not depend on rapidity in the central region (assuming a wide plateau in the rapidity distribution).

Results of the Pisa-Stony Brook collaboration, reported at the Batavia Conference <sup>4),33)</sup> favour the second picture over the first one. This is also what one may conclude from the recent results of the CERN-Hamburg-Vienna collaboration <sup>25)</sup> which analyzed charged-neutral ( $\gamma$  ray) correlations. Data at two different energies,  $\sqrt{s} = 31$  and  $53$  GeV, are shown in Fig. 10a. Fixing the charged particle rapidity at  $y_1 = 0$  and  $2.5$ , respectively, one sees that the two-particle distribution shows a pronounced

maximum when  $y_2 = y_1$  (clear short-range effects). Furthermore, the double distribution, as well as the single one, are not much energy dependent and any rising behaviour cancels out when calculating  $R$  <sup>43)</sup>. As the rapidity of the charged particle is chosen in the fragmentation region, one sees an important change in shape and in magnitude of the correlation distribution from that observed at low centre-of-mass rapidity. Important long-range effects are obviously present also. One may also notice the energy dependence of the correlations observed in the fragmentation region as opposed to the scaling behaviour met in the central region. Figure 10b shows some new results from the Pisa-Stony Brook experiment <sup>25),33)</sup>. They correspond to charged-charged correlations in the central region. One sees again that the observed correlations have a clear short-range character but that the shape and the magnitude of the correlation function change with  $y$  in an important way beyond  $|y| = 1$ , thus disclosing an important long-range effect. The very close relation of the charged-charged and charged-neutral correlations should be stressed <sup>44)</sup>. The magnitude of the correlation function is in both cases of the order of 60-70%. This should be considered as important.

In order to realize this, one may consider the typical positive short-range correlation associated with the formation of a  $\rho$  meson. It is only 10% and this has to do with the actual rapidity density which is found (about two for charged particles). Knowing that a second particle should be within two to three units of rapidity of the first one, as expected from  $\rho$  decay, does not enhance much expectation based on average density. Associating all the observed correlations to particle clustering along a multi-exchange chain (short-range correlation only), the observed effect would call for mean cluster multiplicities of five to seven <sup>45)</sup>. This is more than expected in any simple picture. This puzzle is, however, partly resolved by the presence of important long-range effects which should leave to the actual short-range clustering effect, clearly seen in Figs. 10a and 10b, only part of the observed effect.

Before we turn to this, we may illustrate once more the interplay of short-range and long-range effects with recent results from the CERN-Hamburg-Vienna collaboration <sup>25)</sup> shown in Fig. 11. One sees the inclusive  $\pi^0$  distributions measured for different numbers of charged pions observed within a specific (fragmentation) rapidity interval. One sees that the mean number of  $\pi^0$  in the same interval rises with the number of observed  $\pi^\pm$  (clear short-range effect). One sees also that the observation of a particular number of  $\pi^\pm$  has an important implication for the  $\pi^0$  rapidity distribution over the whole range of rapidity (clear long-range effects).

## 6. - DIFFRACTIVE EXCITATION

The typical process (described in terms of the most frequent rapidity distribution in Fig. 9b), which one may consider to describe the observed short-range correlation effects, is much different from an obvious diffractive excitation mechanism whereby one proton fragments in a relatively small number of secondaries while the other one is merely quasi-elastically scattered. This a priori results in a rapidity distribution, as shown in Fig. 9d. The semi-classical description here used is adequate when such a phase space configuration holds. Diffractive excitation is well known at PS energy <sup>32),46)</sup>. However, the available rapidity range is so small that such a clear separation is possible only for relatively low excitation masses (or very low multiplicities). Going any further requires a model calculation. With increasing energy, it becomes easier to separate quasi-elastically scattered protons off a proton target, which is excited even to a relatively high mass, from the fragment protons of an excited projectile. Evidence for such phase space configurations at ISR energy demonstrates the energy independence of such processes, as expected from diffractive phenomena. It is also possible to determine how such diffractive processes extend in missing mass and multiplicities.

Figure 12a shows the proton distribution at fixed  $p_T = 0.8 \text{ GeV}/c$ , observed by the CERN-Holland-Lancaster-Manchester collaboration. It shows a strong quasi-elastic peak (elastic scattering has been excluded here) which can safely be labelled as a diffractive excitation effect. There is a clear separation between a peak at  $x > 0.95$ , corresponding to a quasi-elastically scattered proton, from a plateau at  $x < 0.95$ , associated with protons from fragmenting proton projectiles. This forward peak appears as relatively stable with increasing energy across the whole ISR energy range. This is new from what was already known at the time of the Batavia Conference <sup>4)</sup>. Once such single diffractive processes (as opposed to diffractive excitation of both protons, which could also be present, though more difficult to detect) are demonstrated many questions arise.

It is very important to know the total cross-section associated with such a production process. Data are, however, available only at relatively large  $p_T$  (large  $|t|$ ) and nothing urges us to continue down to  $t_{\min}$  the exponential  $t$  behaviour, with slope  $3-4 \text{ GeV}^{-2}$  measured by the CERN-Holland-Lancaster-Manchester collaboration and the Aachen-CERN-Genova-Harvard-Torino collaboration <sup>47)</sup>. One may tentatively say that the cross-section

attached to single diffractive excitation is as large as total elastic scattering <sup>48)</sup>. It is very difficult to go to lower  $|t|$  values at ISR. This is a question for which results at NAL at low  $|t|$  should be extremely useful <sup>49)</sup>. It is also interesting to study the missing mass distribution to the quasi-elastic peak. The approximate scaling behaviour suggests that  $d\sigma/dM \sim M^{-1}$  near the dip of the  $x$  distribution (Fig. 12) where the missing mass is of the order 10 GeV. In any case the fact that diffractive excitation extends over such a large range of masses is by itself an important discovery. This is also found by the Aachen-CERN-Genova-Harvard-Torino collaboration <sup>47)</sup> who further indicates that the multiplicity associated with a quasi-elastically scattered proton extends to relatively large values. Diffractive excitation, as thus clearly seen, still involves relatively small multiplicities as compared to average multiplicity at ISR energies. Nevertheless, the recoil mass is seen to be sometimes associated to charge multiplicity up to six and even more. Studying such a process in more detail is very important as it shed light on proton excitation much beyond the well-known resonances.

The next point refers to the rapidity distributions met in such reactions. One would expect an important rapidity gap between the quasi-elastically scattered proton and the fragments of the other one, as implied by Fig. 9d. That the actual configuration is indeed such is suggested by Fig. 12b which shows the pion rate at  $90^\circ$  observed as a function of the proton momentum. There is an important  $x$  region, where the observed proton carries away a lot of energy but yet not enough to be clearly quasi-elastically scattered and for which the measured rate at wide angle does not depend practically on the proton momentum. For  $x$  near enough one, however, when the proton is obviously quasi-elastically scattered, the yield at  $90^\circ$  drops dramatically, as expected from a configuration such as that drawn in Fig. 9d.

Diffractive excitation is naturally associated with Pomeron exchange which favours by its maximal intercept such a large rapidity gap. It is then very interesting to compare Pomeron proton scattering, as thus measured, to proton-proton scattering measured at the same energy. Is the mean multiplicity, associated to a missing mass  $M$  in a clear diffractive event, similar or much different from that measured in proton-proton collisions at centre-of-mass energy  $M$  ? Are also correlations among the fragment particles similar or much different from those measured in proton-proton collisions ? To the extent that the relatively small number of secondaries obtained in high energy reactions is associated with a leading particle effect, one could expect mean multiplicities in Pomeron proton collisions to be larger than in proton-proton collisions. This fact is of course also related to the presence, or not, of double Pomeron exchange. Studying in detail the recoiling hadronic system obtained in such quasi-elastic collisions is therefore very interesting.

Single diffractive excitation, as now seen, has important implications on wide angle correlations. If a cross-section as high as  $\sigma_{el}$  is attached to rapidity configurations as sketched in Fig. 9d, observing a wide angle secondary, implies that the corresponding event is not of a single diffractive type, which contributes zero practically to the mean rapidity distribution at low centre-of-mass rapidity. The probability of observing another secondary at wide angle is therefore enhanced by at least 25% from what expected from the single particle distribution alone. This is a typical and important positive long-range correlation effect, which decreases by as much the amount of correlation to be attributed to actual clustering among wide angle secondaries<sup>45)</sup>. Such an effect may not be the only one. The  $90^\circ$  yield observed in association with a relatively energetic proton ( $x > 0.5$ ) is typically 20% below the average value<sup>25)</sup>, when it conversely increases, of course, much above average when one requires on the contrary a relatively slow proton ( $x < 0.5$ ). This should be considered also as an important long-range effect, the observation of a wide angle secondary being a slight but actual bias against those reactions with a leading proton. The interplay between long-range and short-range effects in the correlations of Figs. 10a and 10b is not yet fully resolved. This should require much attention since the actual amount of short-range correlations proper among wide angle secondaries is a very important quantity. In plain words it tells us how the vacuum, once perturbed by the encounter of two high energy proton, deexcites itself into pions relatively well separated from obvious proton fragments.

## CONCLUSION

Even though this review contains many recent and interesting results it appears first of all as a status report in an exploration of hadronic processes at very high energies which is just beginning. We have so far only fragmentary information but we can already be confident that the ISR is an appropriate instrument to continue this research in detail, an endeavour which is obviously called for. Even if exotic particles do not show up, though we may still hope they will, one may already foresee several years of extremely exciting research.

ACKNOWLEDGEMENTS

This review would simply not have been possible without the active interest which the ISR groups took in the discussion sessions which were held through the winter months. This review is only a modest survey of all the work and effort which they accepted to make in order to make these meetings worth while. By the same token, the data presented here should be considered as semi-quantitative illustrations. The experimental collaboration(s) listed below each figure number should be consulted before any definite conclusion is drawn.

REFERENCES

- 1) "Tel le geai paré des plumes du paon" according to a French saying  
(as the jay wearing the feathers of the peacock).
- 2) J. Sens - Invited talk, Oxford Conference (1972).
- 3) G. Giacomelli - Rapporteur talk, Batavia Conference (1972).
- 4) M. Jacob - Rapporteur talk, Batavia Conference (1972).
- 5) D. Horn - Physics Reports 4C, 1 (1972).  
For a comprehensive review of recent results, one may consult :  
"Scaling and the Approach to Scaling", ISR Discussion Meeting 3,  
CERN Internal Report (January 1973).  
Look for coming preprints by the CHLM-S.S.-C.B. and B.S. collaborations.
- 6) Experiments at ISR have been so far performed with coasting beams of  
11, 15, 22, 26 and 31 GeV/c, respectively. This spans the range  
250-2000 GeV when expressed in terms of stationary target expe-  
rimentation. This energy range will be referred to as ISR  
energies. Note the overlap with the NAL energy range.
- 7) S. Berman, J. Bjorken and J. Kogut - Phys.Rev. D4, 3388 (1971) ;  
M. Jacob and S. Berman - Phys.Rev.Letters 25, 1683 (1970) ;  
F. Gunion, R. Blankenbecler and S. Brodsky - Phys.Rev. D6, 2652 (1972) ;  
F. Low and S. Treiman - Phys.Rev. D5, 756 (1972) ;  
J. Polkinghorne and P. Landshoff - Physics Reports 5C, 1 (1972) ;  
J. Kogut and D. Susskind - Physics Reports, to be published (1973).
- 8) For a review of the Froissart bound constraints and Regge models pre-  
dictions, see :  
P.D.B. Collins - Physics Reports 1C, 103 (1971), and  
S.M. Roy - Physics Reports 5C, 125 (1972) ;  
For a review of Reggeon calculus predictions with cross-sections rising  
to a limiting value, see :  
A. Tavkhelidze - Rapporteur talk, Kiev Conference (1971) ;  
For QED inspired models, see :  
H. Cheng and T.T. Wu - Phys.Rev.Letters 24, 1456 (1970),  
and related papers.

- 9) Present information, as obtained by the Argonne-Bologna-CERN Collaboration, the British-Scandinavian Collaboration and the CERN-Holland-Lancaster-Manchester Collaboration are summarized in Ref. 5).
- 10) J. Benecke, T.T. Chou, C.N. Yang and E. Yen - Phys.Rev. 188, 2159 (1969) ;  
C.N. Yang - "High Energy Collisions", Gordon and Breach, New York (1969) ;  
R.P. Feynman - Phys.Rev. Letters 23, 1415 (1969) and "High Energy Collisions"  
op. cit. ;  
K. Wilson - Acta Phys. Austriaca 17, 37 (1963).
- 11) The rapidity  $y$  of a secondary is defined as  $y = \frac{1}{2} \log(E + p_L / E - p_L)$ .  
The particular interests presented by such a variable are well known <sup>2),4)</sup>. One should stress that, instead of  $y$ , one has often to use  $\eta = -\log \operatorname{tg} \theta/2 = \frac{1}{2} \log(p + p_L / p - p_L)$ , when only the production angle of the secondaries can be measured. At present this is very often the case. Such an approximation is good except for very energetic (small angle) or relatively slow (wide angle) secondaries. In the latter case  $dc/d\eta$  at  $\eta=0$  should be typically 20% below the actual value of  $dc/dy$  at  $y=0$ . In this review we will use rapidity for both  $y$  and  $\eta$ . The range of validity of the approximation of using  $\eta$  instead of  $y$  is clearly seen on recent 200 GeV pp data (J. Whitmore, private communication).
- 12) A group of secondaries (cluster), isotropically distributed in their centre-of-mass system, shows a rapidity spread directly related to the corresponding  $p_T$  distribution. Using a Gaussian shape, one is led to a rapidity spread of about two units. This is the strongest clustering effect which one may expect in view of the actual width of the  $p_T$  distribution. Any expected dynamical effect (spin alignment, small momentum transfer...) will tend to further extend in rapidity such a minimal cluster size.
- 13) Scaling is, of course, tested at best to a 10% level. If total cross-sections increase, there is no reason to expect that scaling should hold precisely. When we speak about scaling, it is therefore up to logarithmic terms which could be similar to those attached to the observed rise of  $\sigma_{tot}$ .

- 14) B.J. Blumenfeld et al. - Contribution to the APS Meeting, New York (1973).  
The lack of scaling shown by the results presented at the Batavia Conference <sup>2),3)</sup> should be considered with some care since part of the effect could be due to triggering selection. I am indebted to L. Litt for a discussion of that question.
- 15) With present statistics one cannot differentiate well enough a  $\pi^+$  from a  $\pi^-$  behaviour.
- 16) M. Banner et al. - Phys.Letters 41B, 547 (1972), contribution to the Batavia Conference (1972).
- 17) For a comprehensive review of recent results on large transverse momentum phenomena, one may consult ISR Discussion Meeting 2, CERN Internal Report (December 1972). Look for coming preprints by S.S., C.C.R., P.SB and B.S. Collaboration.
- 18) P. Landshoff and J. Polkinghorne - DAMTP Cambridge Preprints (1972-1973).
- 19) D. Amati, L. Caneschi and M. Testa - CERN Preprint 1597 (1972).
- 20) See also :  
R. Blankenbecler et al. - SLAC Preprints (1972).
- 21) In a more general way, one may not explicitly consider an elementary particle exchange but assume Bjorken scaling for an amplitude with one particle far off shell. This, of course, indirectly assumes a point-like interaction somewhere.
- 22) It should be borne in mind that if we considered individual secondaries, the theoretical picture can just as well be phrased in terms of small clusters of secondaries with arbitrary spins fragmenting into the actually observed particles.
- 23) In the model of Ref. 19), in particular, scaling is reached much more quickly in the fragmentation region than in the central region. What matters there is  $p_T^2/s$  when  $p_T/\sqrt{s}$  terms are explicitly present in the central region ( $x=0$ ).
- 24) For a review of the parton picture of elementary particle, see :  
J. Kogut and L. Susskind - Ref. 7), and, of course :  
R.P. Feynman - Lecture Notes, Benjamin (1973).

- 25) For a review of present results, one may consult : "Two-Body Correlations and Associated Multiplicities", ISR Discussion Meeting 4, CERN Internal Report (February 1973). Look for coming preprints by P.SB and C.H.V. Collaboration.
- 26) U. Amaldi et al. - CERN NP Preprint (January 1973). CERN-Rome.
- 27) S.R. Amendolia et al. - CERN NP Preprint (February 1973). Pisa-Stony Brook.
- 28) In this review the results of Refs. 26) and 27) only will be considered. It should be kept in mind that some discrepancy exists with results of the Aachen-CERN-Genova-Harvard-Torino Collaboration reported at the Batavia Conference, Ref. 3). This merely underlines the difficulties attached to such measurements. Rather than taking side, we here consider only the results indicating a rise of the total  $pp$  cross-section and explore the consequences which can be drawn for other measurements. The fits presented are casual ones to the extent that we do not consider first a scattering amplitude with correct analytic and crossing properties and then calculate the cross-section. The over simplified approach considered here is enough for the sake of the argument.
- 29) In the fit of Fig. 7, the  $P'$  contribution would be almost three times that of the  $w$  instead of being equal to it as required by exchange degeneracy.
- 30) J. Fischer and C. Bourrely - Private communication.
- 31) S.M. Roy - Physics Reports 5C, 125 (1972).
- 32) F. Zachariasen - Physics Reports 2C, 1 (1971).
- 33) "Correlations at Wide Angle", ISR Discussion Meeting 1, CERN Internal Report (November 1972). Look for coming preprints by P.SB Collaboration.
- 34) Neglecting small transverse momenta, (longitudinal) momentum ratios are related to rapidity differences. One is therefore led to put much weight on the rapidity difference  $\Delta y = |y_1 - y_2|$  of the two observed particles and to discuss the range (in rapidity) of such correlations.

- 35) The range available for secondaries extends with the rapidity difference of the two incident protons, namely  $\log s/m^2$ , which, typically four at PS energy, becomes typically eight at ISR energy. As previously discussed in Ref. 12), a short-range effect extends over two to four units of rapidity, at least two, which corresponds to the  $p_T$  distribution width. ISR energies are therefore a priori sufficient to clearly distinguish short-range from long-range effects when this is hardly possible at PS energy, as discussed in Ref. 4).
- 36) A.H. Mueller - Phys.Rev. D2, 2963 (1970).
- 37) With a non-factorizable leading  $J$  plane singularity, one should also expect long-range correlations. Again the short-range nature of such correlations, as even scaling, should be good only up to logarithmic terms.
- 38) In this Regge approach, correlations between  $2\pi^-$  (exotic system) should extend over a shorter range of rapidity since the corresponding (exotic) effective intercept should be lower than  $\frac{1}{2}$ . This is an interesting question for the split field magnet study.
- 39) As discussed in Ref. 4), the same effect is already clearly seen at 30 GeV (results from the Brookhaven-Vanderbilt group). It is also even more clear on the very recent results on  $\pi^-$  semi-inclusive distributions at 205 GeV/c of the NAL-ANL collaboration. This is this particular effect which was emphasized and parameterized in the calculation of Ed. Berger et al. - Phys.Rev. D6, 2580 (1972), in terms of the combination of short-range and long-range effects obtained in the model calculation made.
- 40) Secondaries observed at wide angle define inelastic collisions. It is therefore more convenient to normalize rates to  $\sigma_{inel}$  rather than to  $\sigma_{tot}$ , and the more so to the extent that  $\sigma_{el}$  is actually a sizeable fraction (20%) of  $\sigma_{tot}$ .
- 41) Limiting fragmentation corresponds in particular to limiting patterns for rapidity distribution in the neighbourhood of  $y_A$  and  $y_B$ , irrespectively of the extension of the global rapidity interval  $Y$ . See Fig. 9.

- 42) Such a clear separation is of course not yet possible at PS energy with  $y_A - y_B \sim 4$  only.
- 43) It is an important question looking at Pisa-Stony Brook results that the rapidity plateau rises much more (30%) across the ISR energy range than what measured with a spectrometer (Fig. 1a). As already said, this cancels, however, the sharp rise of the double distribution (60%) also reported, when calculating R. We take the attitude that it is partly a spurious effect and that both distributions in effect do not rise very much. This is, however, a point where the split field magnet analysis should provide the required confidence. No definite conclusion can be drawn before this question is fully resolved. In a pure fragmentation model the double distribution at  $y_1 \approx y_2 \approx 0$  would increase by a factor two or so across the ISR energy range when the single distribution would not increase appreciably. See Ref. 4) for a review.
- 44) Recent results from the Pisa-Stony Brook Collaboration give very similar double distributions for  $\nu\bar{\nu}$  at  $y_1 \approx 0$ , see Ref. 25).
- 45) S. Pokorski and P. Pirilä - CERN Preprint TH. 1607 (1972).
- 46) L. Van Hove - Physics Reports 10, 344 (1971).
- 47) G. Goldhaber - Private communication.
- 48) This is the estimate arrived at when including a diffractive component in the analysis of multiplicity distributions.  
J.D. Jackson and C. Quigg - NAL Preprint  
K. Fiałkowski and H.I. Miettinen - Phys.Letters B43, 61 (1973) ;  
L. Van Hove - Phys.Letters B43, 65 (1973).
- 49) Results from the Rutgers group on the one hand, and the Columbia-Stony Brook group on the other hand, should be extremely interesting in that respect. Bubble Chamber results at 100, 200 and 300 GeV/c support a single diffractive cross-section about equal to  $\sigma_{el}$ .

FIGURE CAPTIONS

- Figure 1 a) Inclusive pion distributions at  $x = 0$  for several  $p_T$  values.  
b) Inclusive proton and anti-proton distributions at  $x = 0$  and  $p_T = 0.65$  GeV/c.
- Figure 2 a) Transverse momentum distribution of  $\pi^0$  produced at  $90^\circ$  at  $\sqrt{s} = 53$  GeV. The solid line corresponds to the extrapolation of the low  $p_T$  behaviour.  
b) Large transverse momentum distribution of charged pions produced at  $90^\circ$  at  $\sqrt{s} = 44$  and  $53$  GeV, respectively. The solid line corresponds to the extrapolation of the low  $p_T$  results.
- Figure 3 Increase of the integrated rate ( $3.2 < p_T < 5.2$  GeV/c) with energy for charged pions produced at  $90^\circ$ . The preliminary rate of increase quoted for  $\pi^0$  distribution at large  $p_T$  <sup>3),4)</sup> may have to be reconsidered <sup>14)</sup>. As also seen by the British-Scandinavian-collaboration, the global positive (negative) yield at  $1 < p_T < 3$  GeV/c does not change appreciably between  $\sqrt{s} = 31$  and  $53$  GeV <sup>5)</sup>.
- Figure 4 Production rate of positive and negative secondaries at  $90^\circ$  for different large  $p_T$  values  $1 < p_T < 3$  GeV/c over the range of ISR energy. One notices a slow departure from scaling at large  $p_T$ .
- Figure 5 Transverse momentum distributions of positives and pions as now available. Note the mismatch between the distributions for positives and pions, respectively. The British-Scandinavian results do not indicate any strong effect.
- Figure 6 a) Production amplitude for a large transverse momentum particle in an over-all multiperipheral framework.  
b) Most probable rapidity distribution corresponding to the production of a large  $p_T$  secondary in a multiperipheral process.  
c) Parton-parton scattering. The hard partons have been represented as valence quarks.  
d) The parton configuration after an initial hard parton scattering at wide angle and parton decay.

- Figure 7
- a) Compilation of total cross-section results using CERN-Brookhaven-Serpukhov and NAL data and the values measured by the CERN-Rome and the Pisa-Stony Brook collaborations, respectively. Also shown are two fits to the rising pp cross-section. The total cross-section may rise indefinitely or saturate to a limiting value. The two fits do not include Regge terms which are assumed to contribute 1 mb at 200 GeV in the second case (exchange degeneracy is, of course, abandoned there).
  - b) The slope parameter (Serpukhov and ISR data only).
  - c) The real part to imaginary part ratio R (Fischer and Bourrely).

- Figure 8
- a) Inclusive rapidity distributions for different charged multiplicities.
  - b) Two particle distributions in the central rapidity region. The solid curves correspond to the product of the single particle distributions. The arrow indicates the value of  $\eta_2$  equal to  $\eta_1$ .

- Figure 9
- a) Rapidity distribution in a typical event. The cluster drawn in the centre of the rapidity interval corresponds to positive correlations among wide angle secondaries assumed here to obtain, irrespectively of the fragmentation of the two incident protons.
  - b) Rapidity distribution at higher energy. Clustering increases with more secondaries found and in each event in a relatively limited rapidity interval.
  - c) Rapidity distribution at higher energy. Clustering does not increase. The average number of clusters in each event increases. The single particle inclusive distributions obtained from 9b or 9c, averaged over all observed events could still be the same. The energy independence of the rapidity distribution in the proton rest frame justifies the limiting fragmentation distributions around  $y(A)$  and  $y(B)$ .
  - d) Rapidity distribution for single diffractive excitation.

- Figure 10
- a) Charged-neutral two-body correlations as a function of rapidity and energy.
  - b) Charged-charged two-body correlations as a function of rapidity and energy.

Figure 11 Inclusive distributions of  $\gamma$  rays corresponding to different charged multiplicities found in a particular rapidity interval.

Figure 12

- a) Inclusive proton distribution for high energy proton. Results at fixed  $p_T = 0.8 \text{ GeV}/c$  and different energies are grouped together.
- b) Associated multiplicity at  $90^\circ$  as a function of the leading proton momentum. The rate measured at wide angle is shown together with the inclusive proton distribution.

figure 1-a

Saclay-Strasbourg  
British-Scandinavian

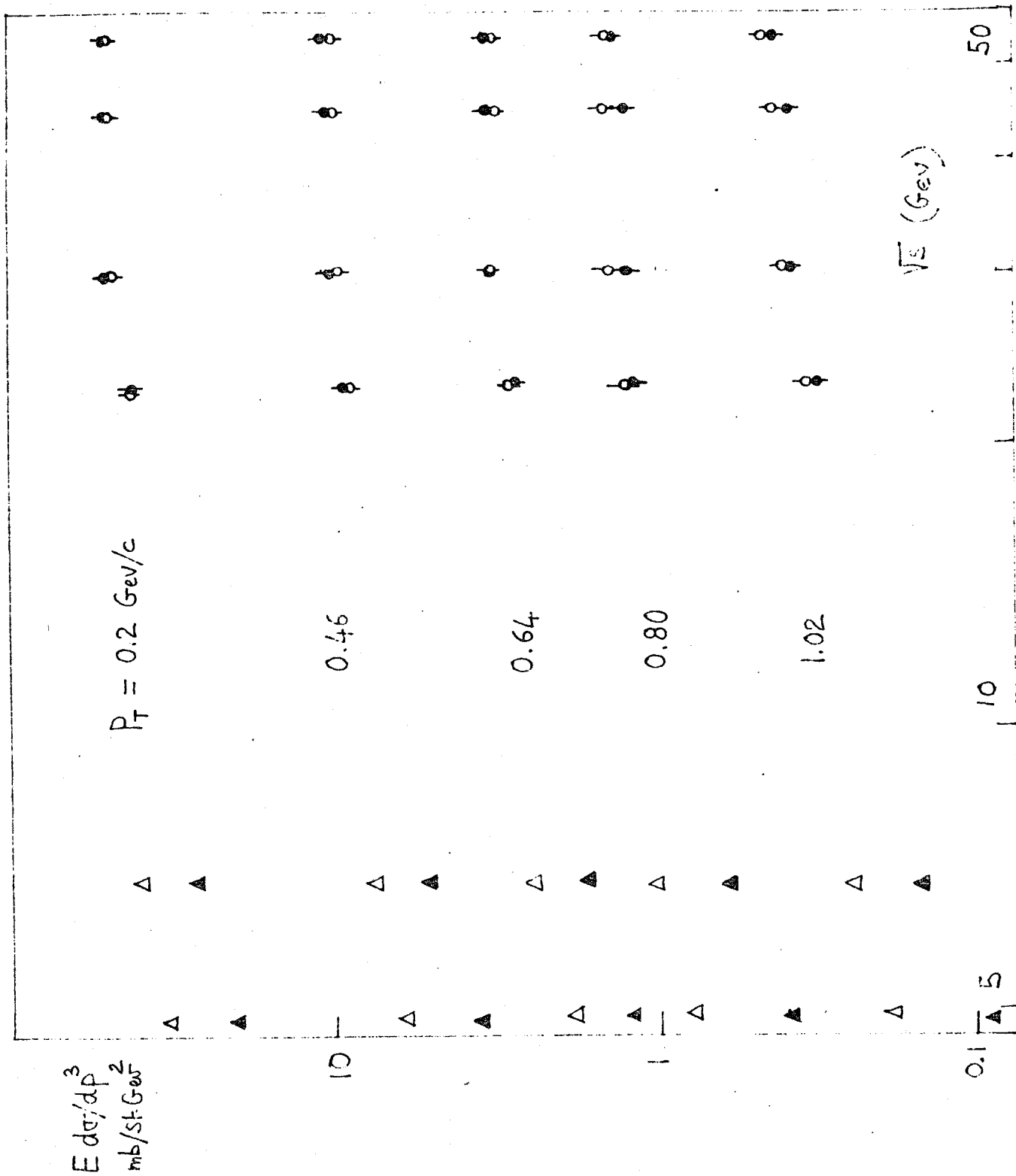
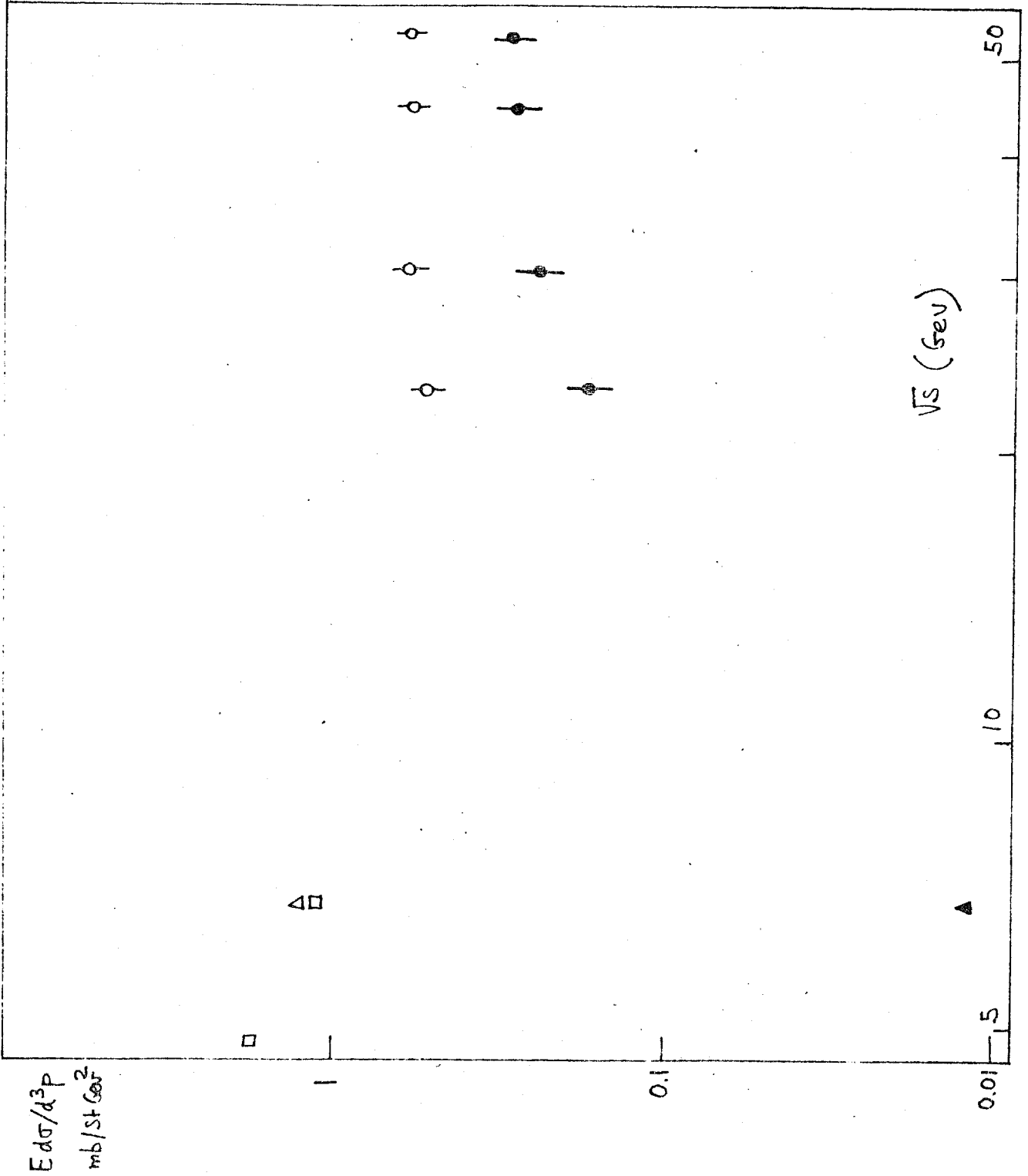


figure 1-b

Saclay-Strasbourg  
(British-Scandinavian)



$$pp \rightarrow p(\bar{p}) + \dots$$

- △ Allaby et al P
- Mück et al P
- Saclay-Strasbourg P
- ▲ Allaby et al  $\bar{P}$
- Saclay-Strasbourg  $\bar{P}$

$$x = 0$$

$$P_T = 0.65 \text{ GeV}/c$$

figure 2-a  
CERN-Columbia-Rockefeller

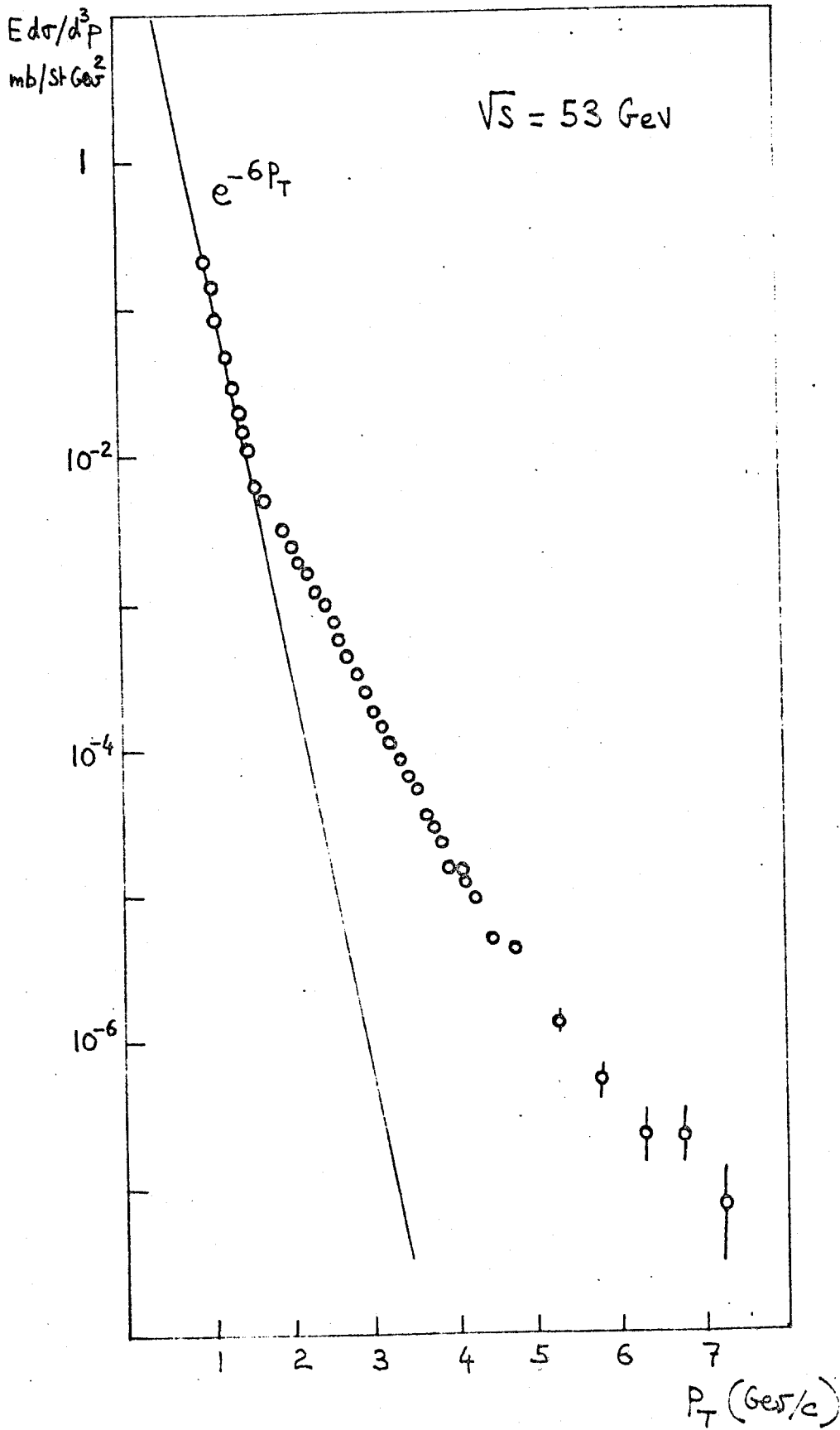


figure 2-b  
Saclay - Strasbourg

PP  $\rightarrow \pi^{\pm} + \dots$

Average

x = 0

●  $\sqrt{s} = 52 \text{ GeV}$

○  $\sqrt{s} = 44 \text{ GeV}$

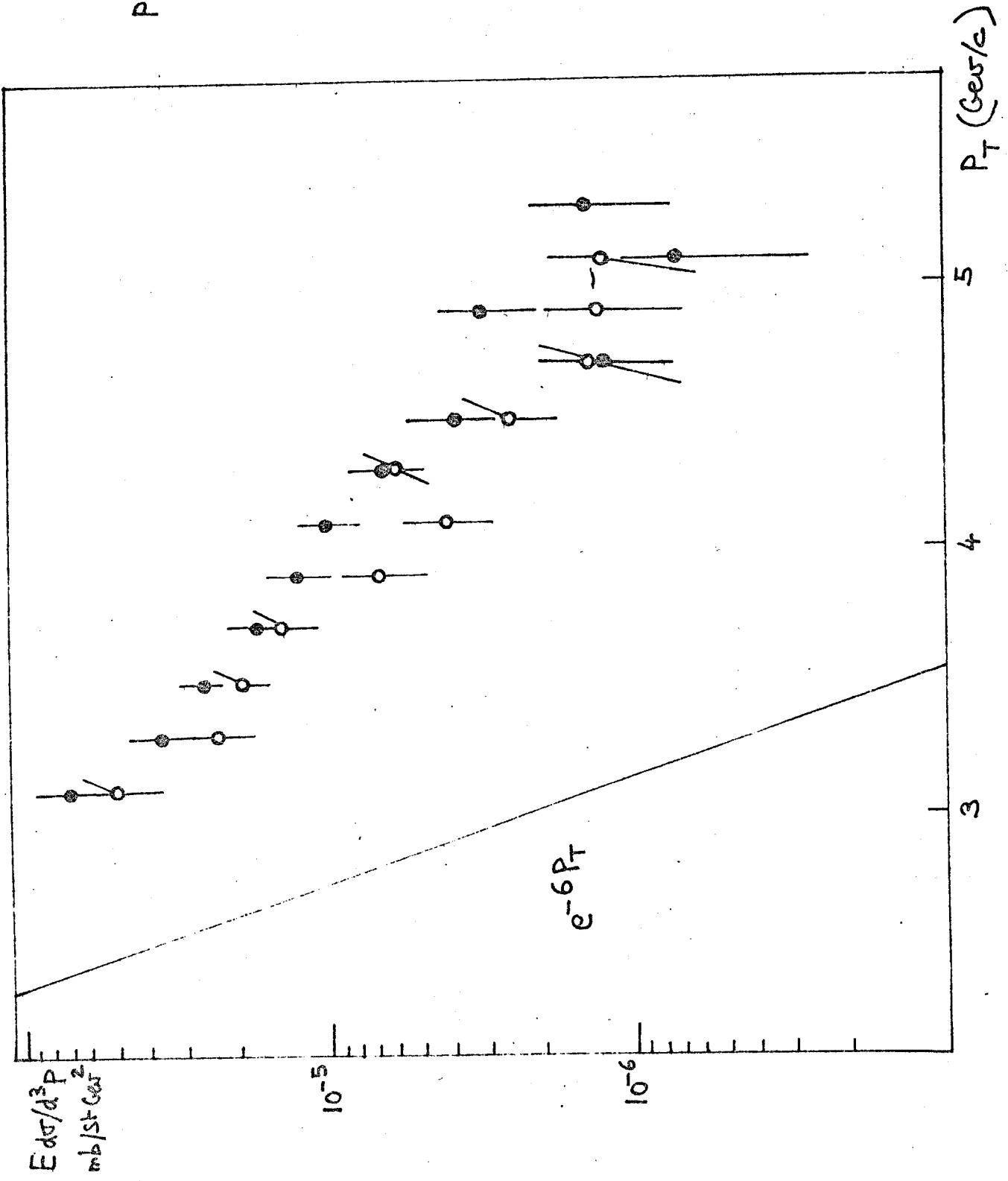
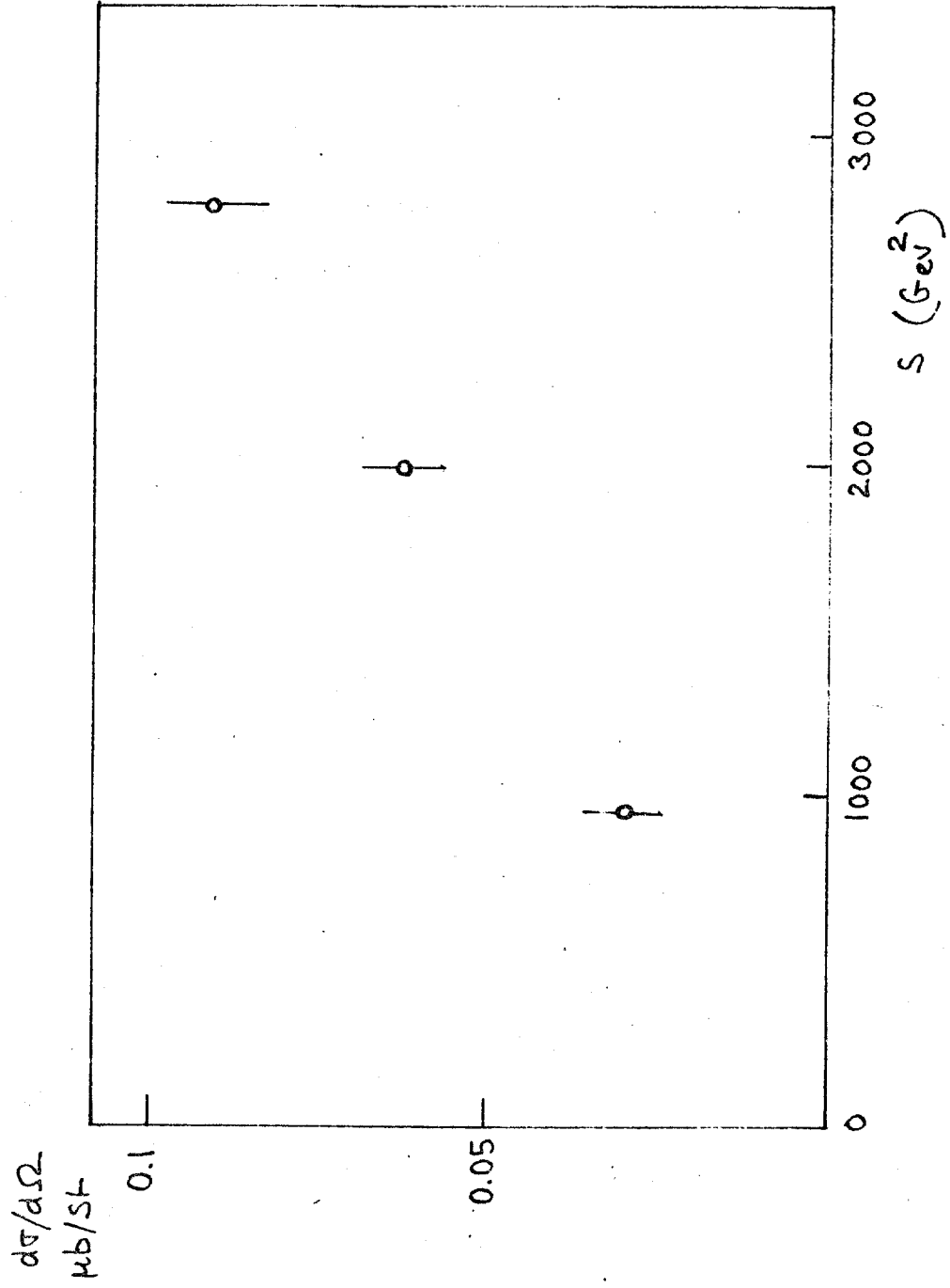


figure 3  
Saclay-Strasbourg



$PP \rightarrow \pi^\pm + \dots$

Average

$3.2 < P_T < 5.2 \text{ GeV}/c$

$X = 0$

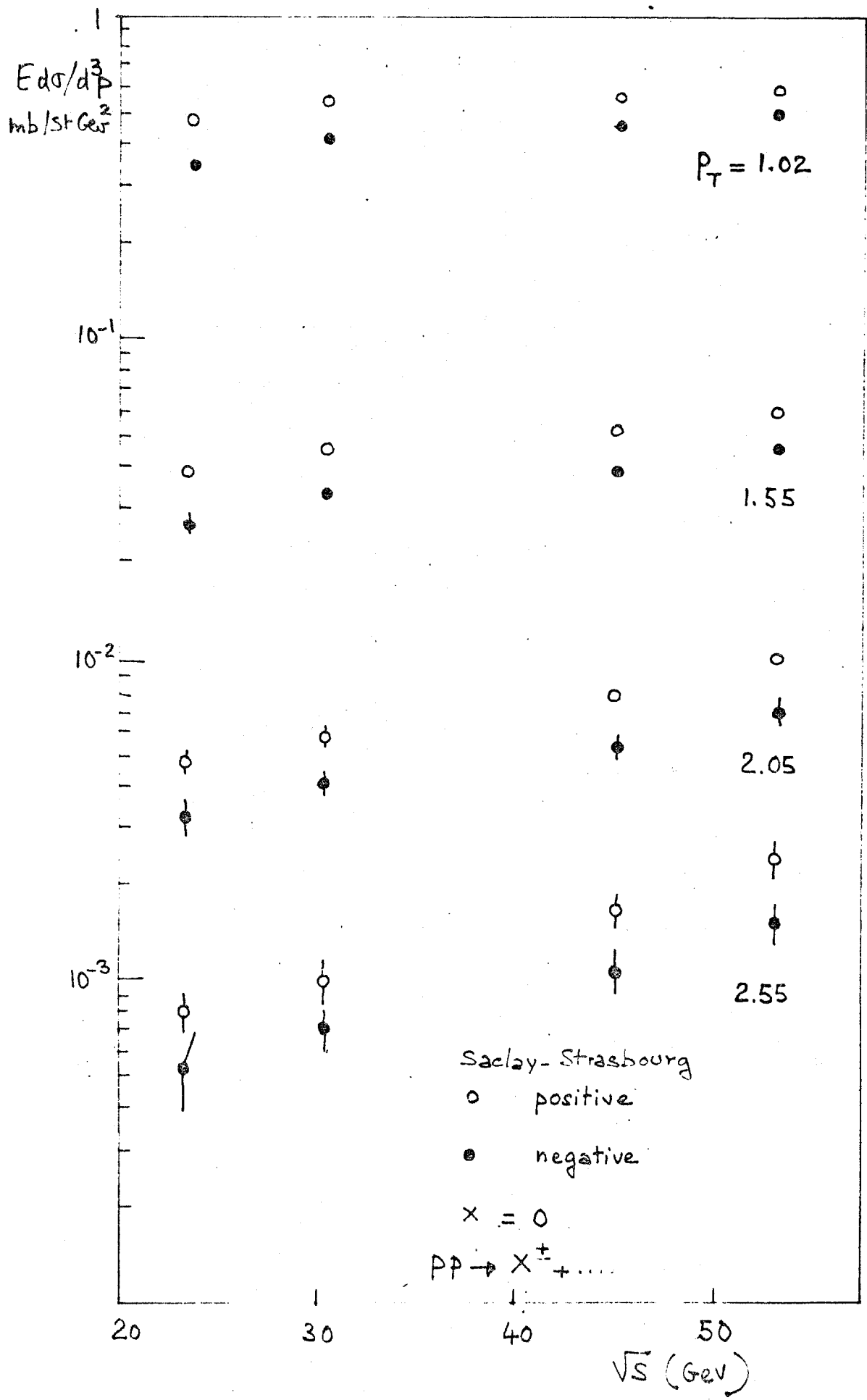


figure 4  
 Saclay-Strasbourg  
 (British-Scandinavian)

$E \frac{d\sigma}{d^3p}$   
mb/st Gev<sup>2</sup>

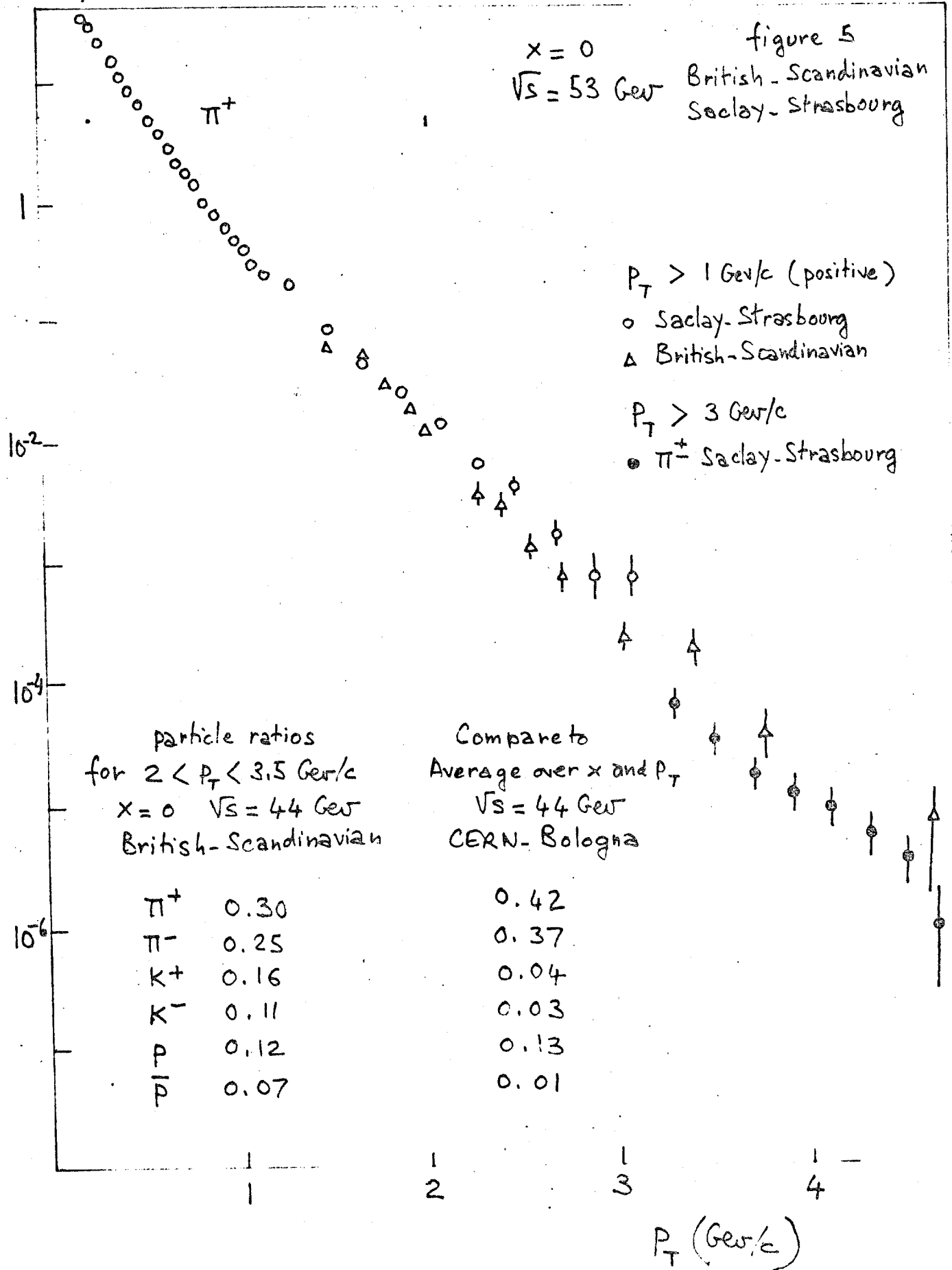


figure 6

$$E ds/dP_L dP_T^2 \sim \left(\frac{1}{P_T}\right)^n F\left(\frac{P_T}{\sqrt{s}}\right)$$

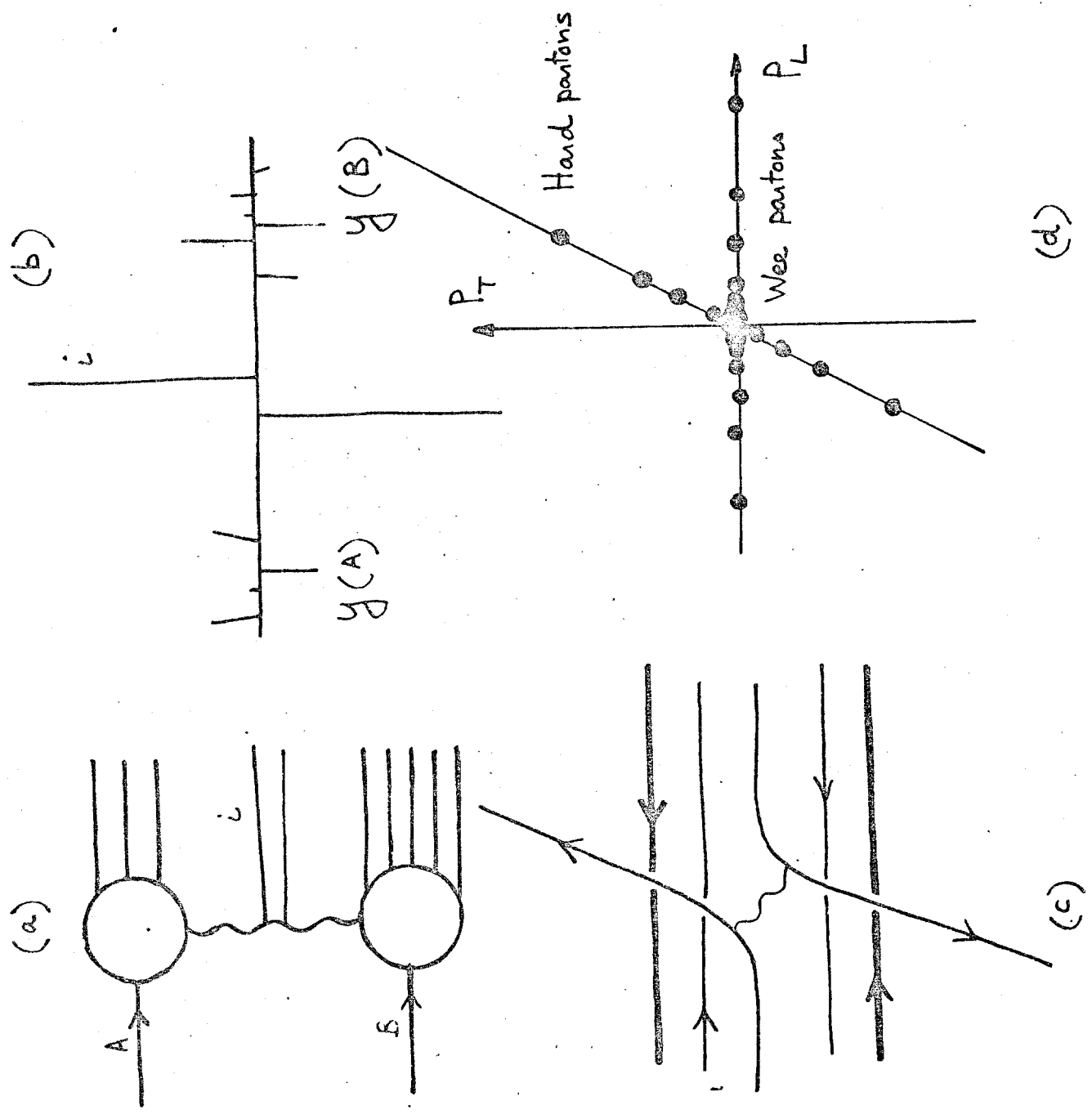


figure 7-a

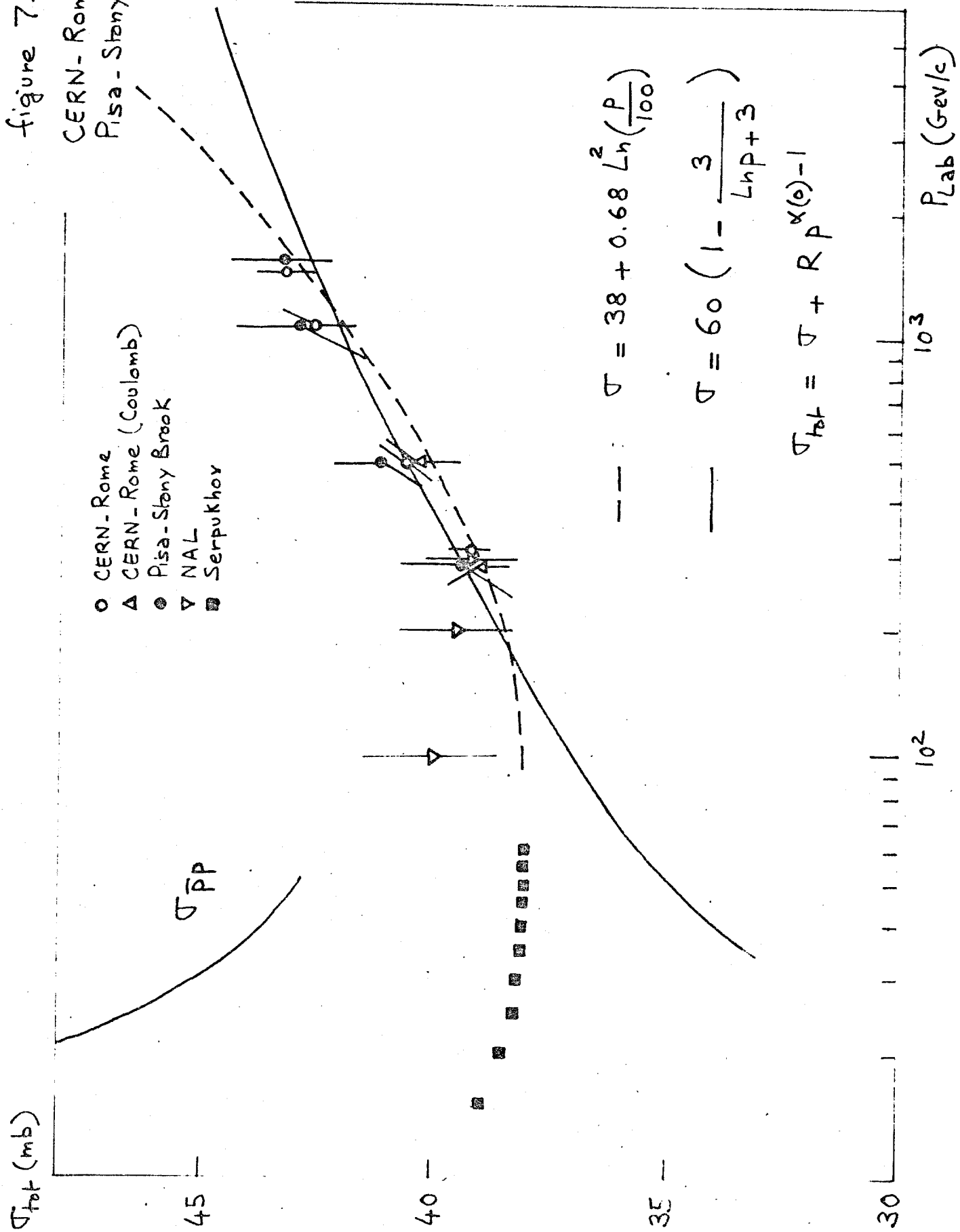
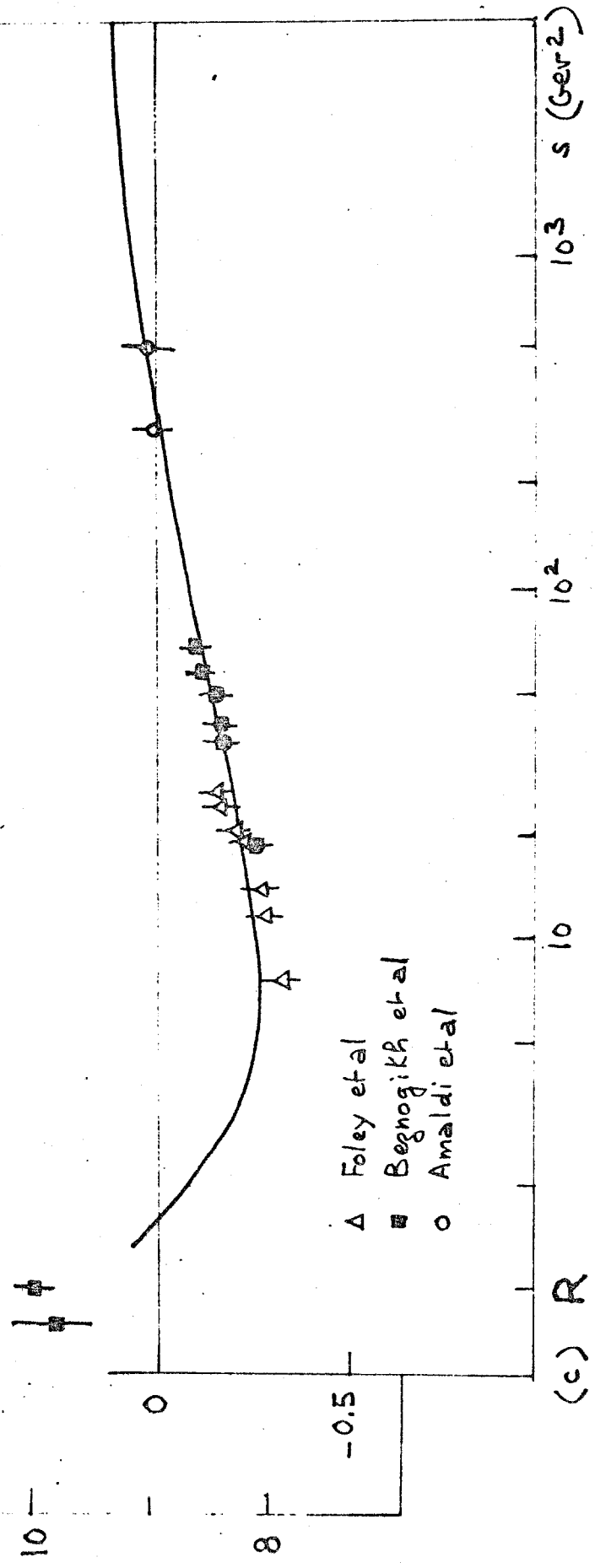
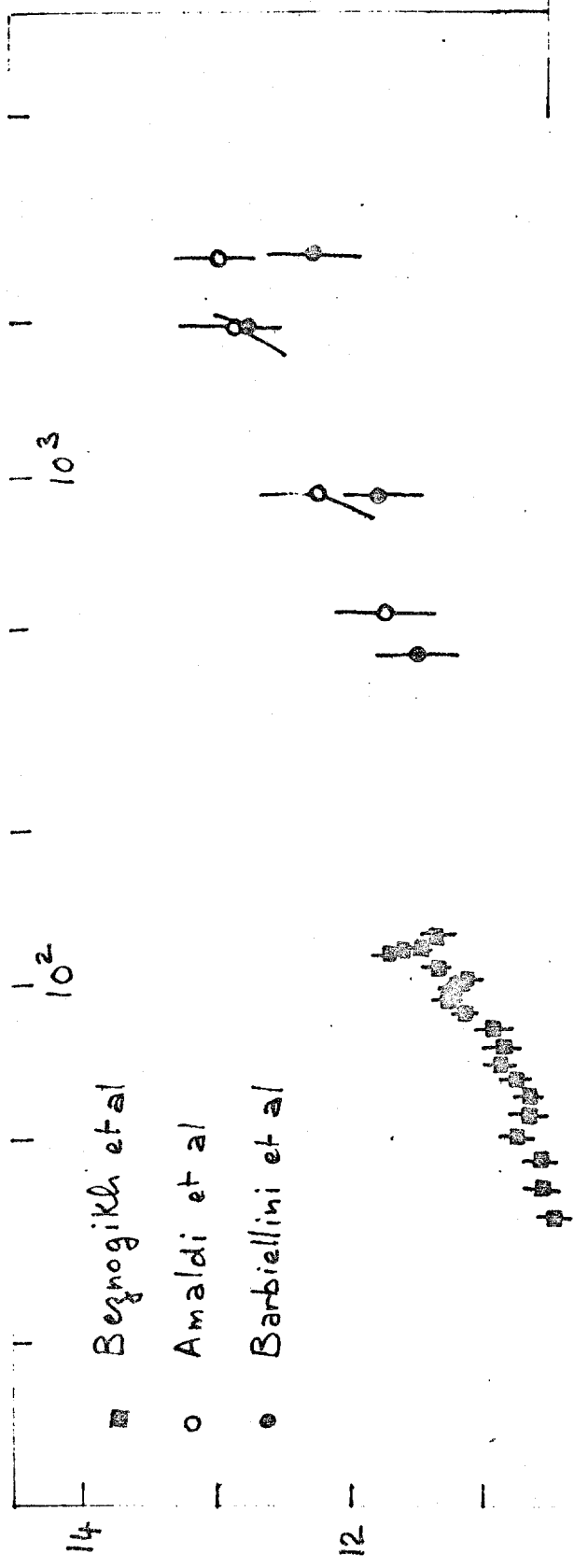


figure 7-b,c

CERN-Rome  
 Aachen-CERN-Genova  
 -Harvard-Torino

$s$  (GeV<sup>2</sup>)

$b$  (GeV<sup>-2</sup>) Slope parameter



(c) R

$$\frac{1}{\sqrt{n}} \frac{d\sqrt{n}}{d\eta}$$

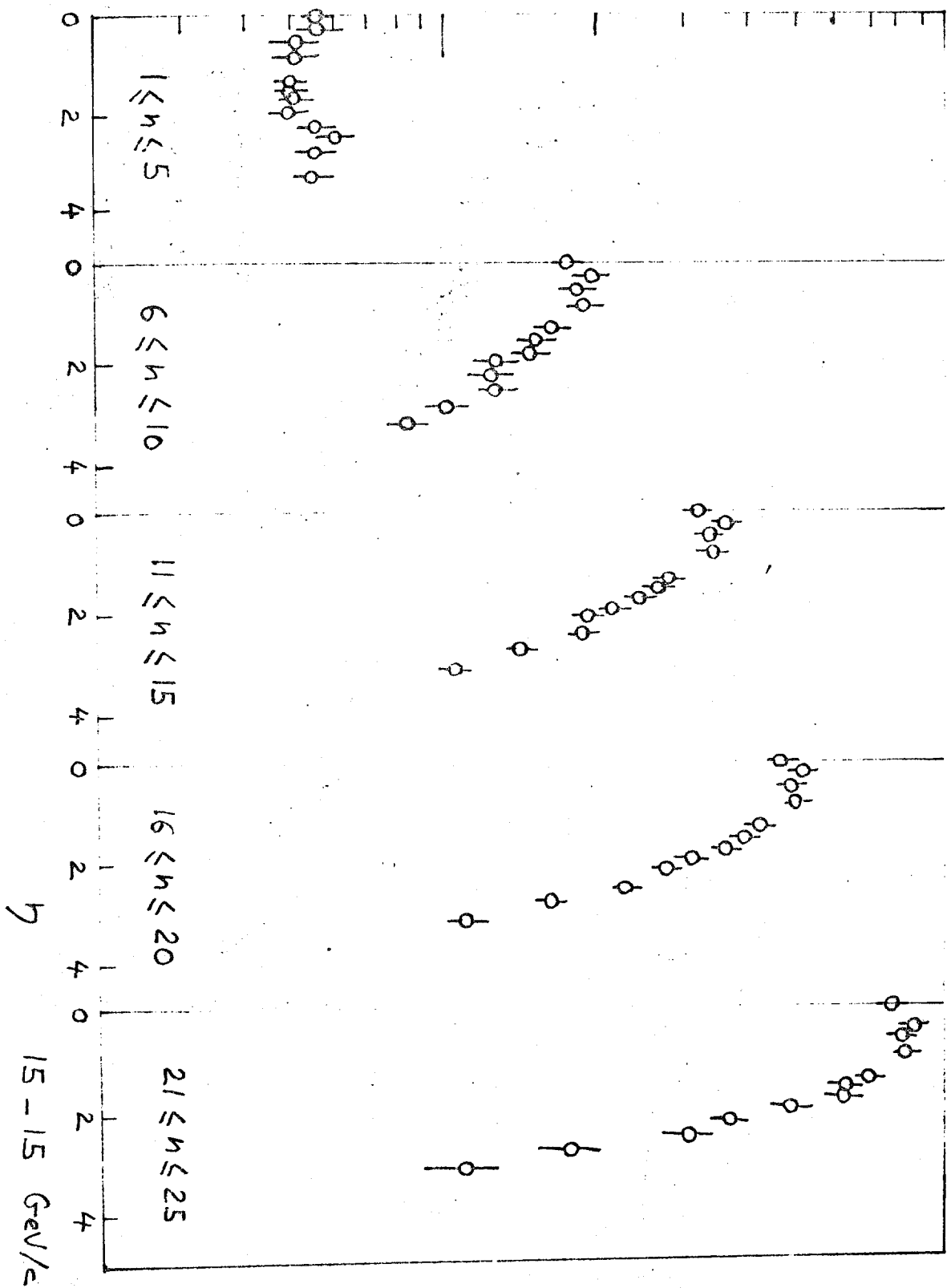


figure 8-a  
Pisa-Strasbourg

two particle distribution  
15-15 GeV/c

figure 8-b  
Pisa-Stony Brook

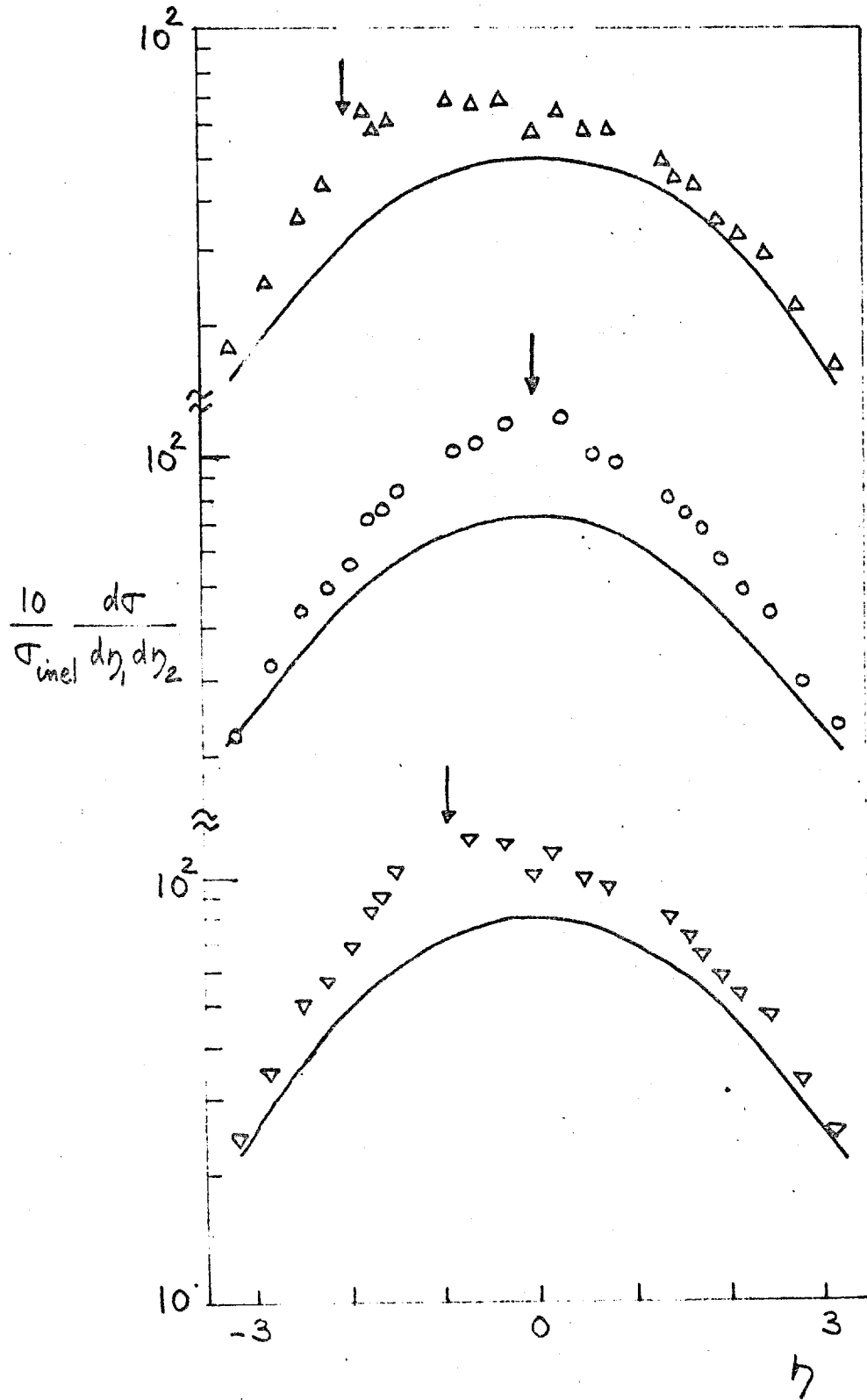
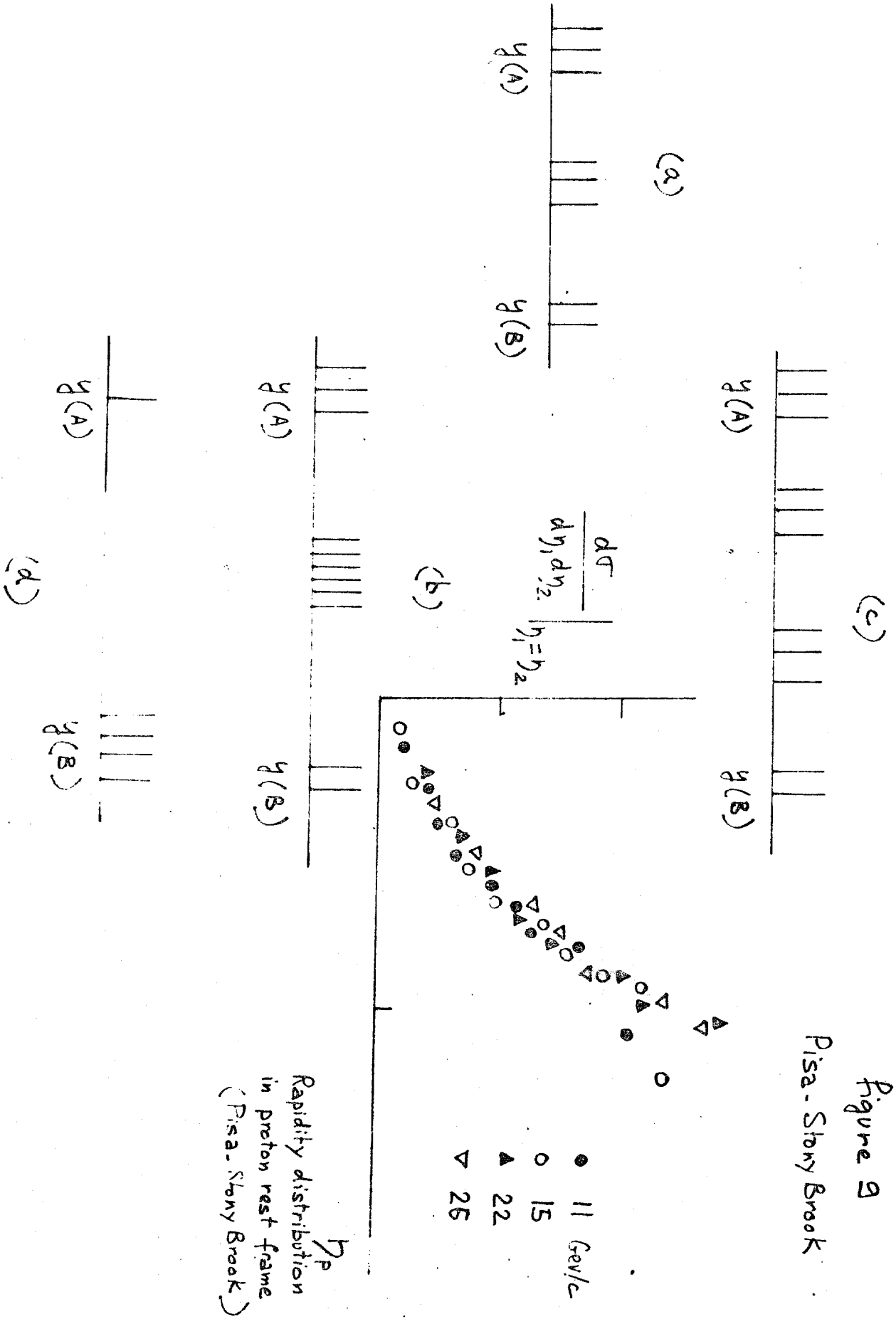


Figure 9

Pisa-Stony Brook



$$R_{12} = \frac{V_{ind} \frac{d\sigma/d\eta_{ch} d\eta_x}{(d\sigma/d\eta_{ch}) (d\sigma/d\eta_x)}}{-1}$$

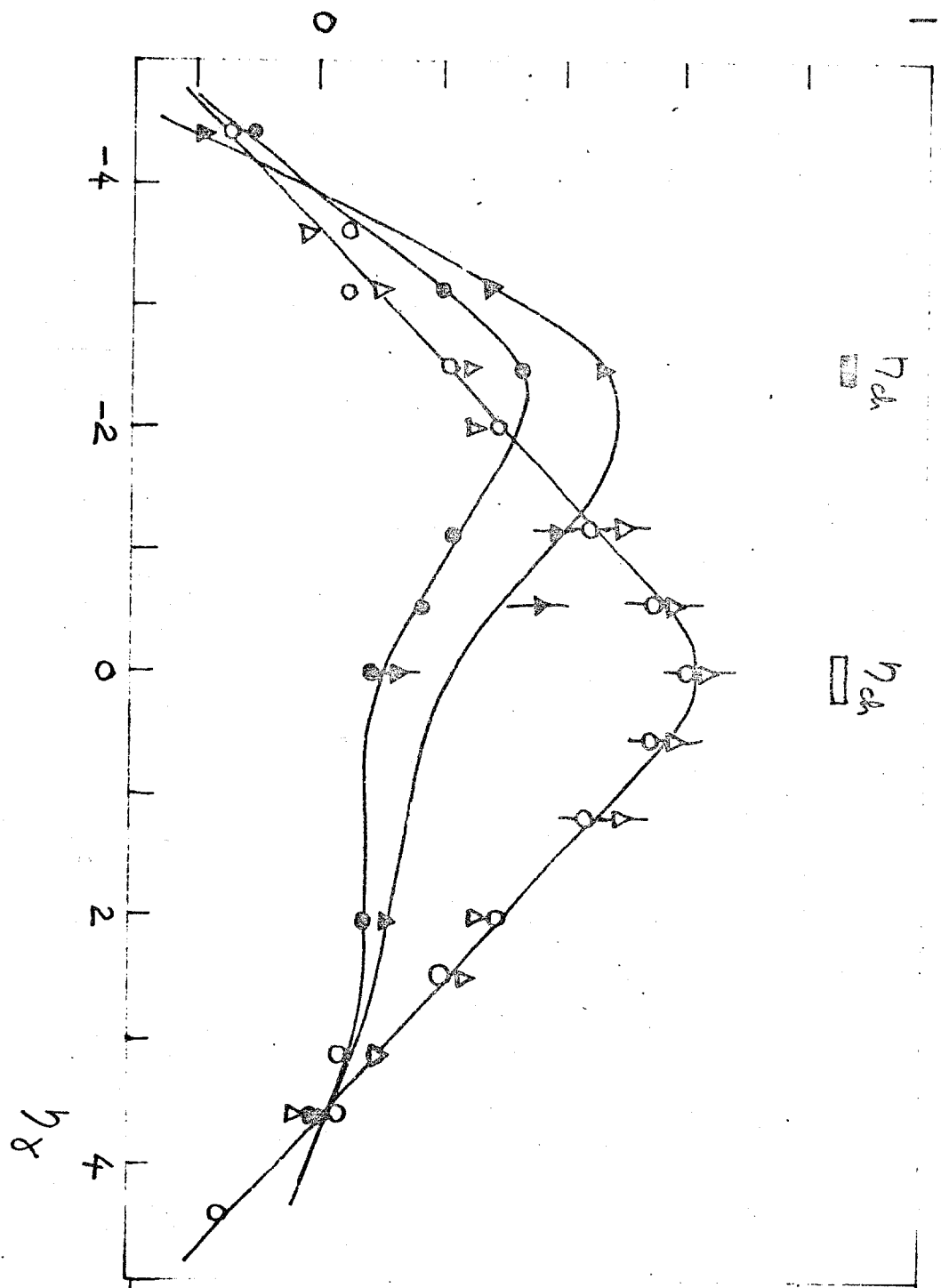


figure 10-a.  
CERN - Hamburg - Vienna

Charged - Neutral  
Correlations  
●  $\sqrt{s} = 30.6$  GeV  
▲  $\sqrt{s} = 53$  GeV

$\eta_1, \eta_2$  dependence 15-15 GeV/c

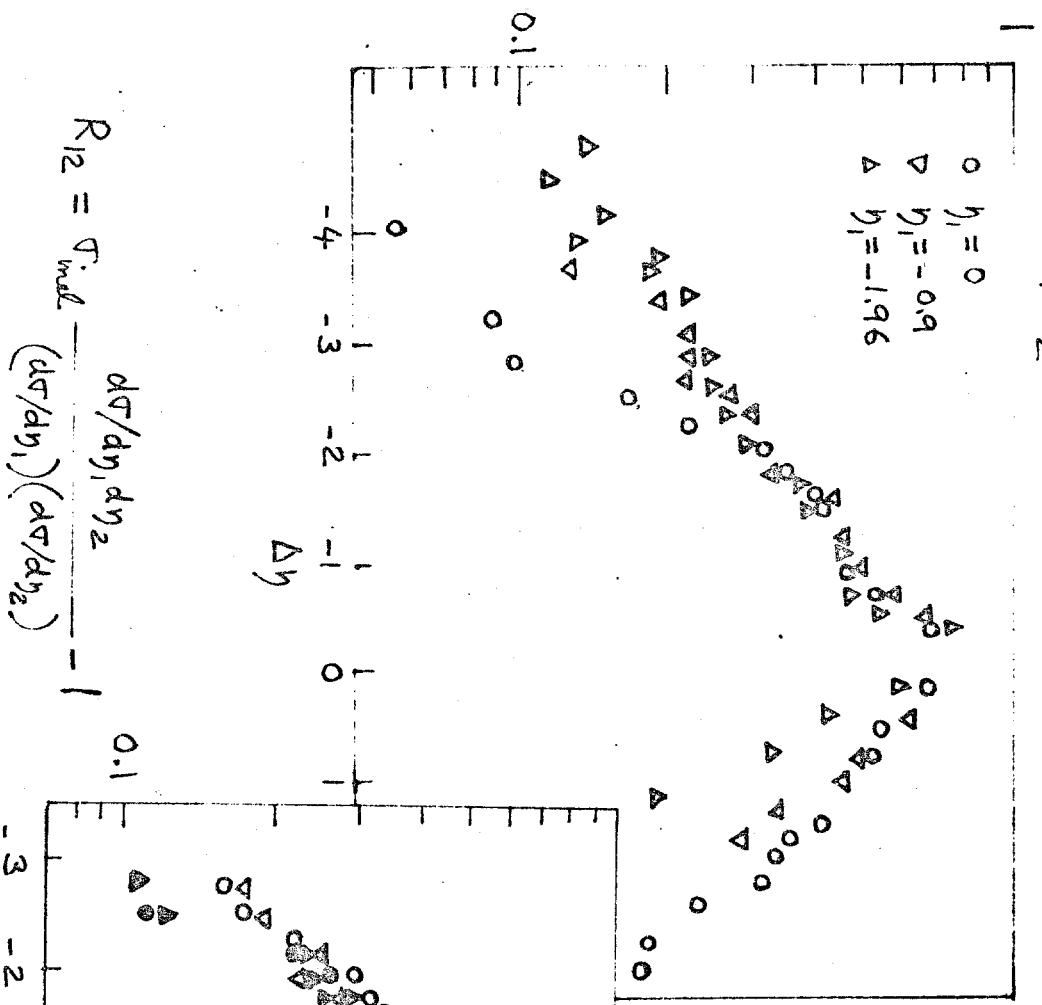
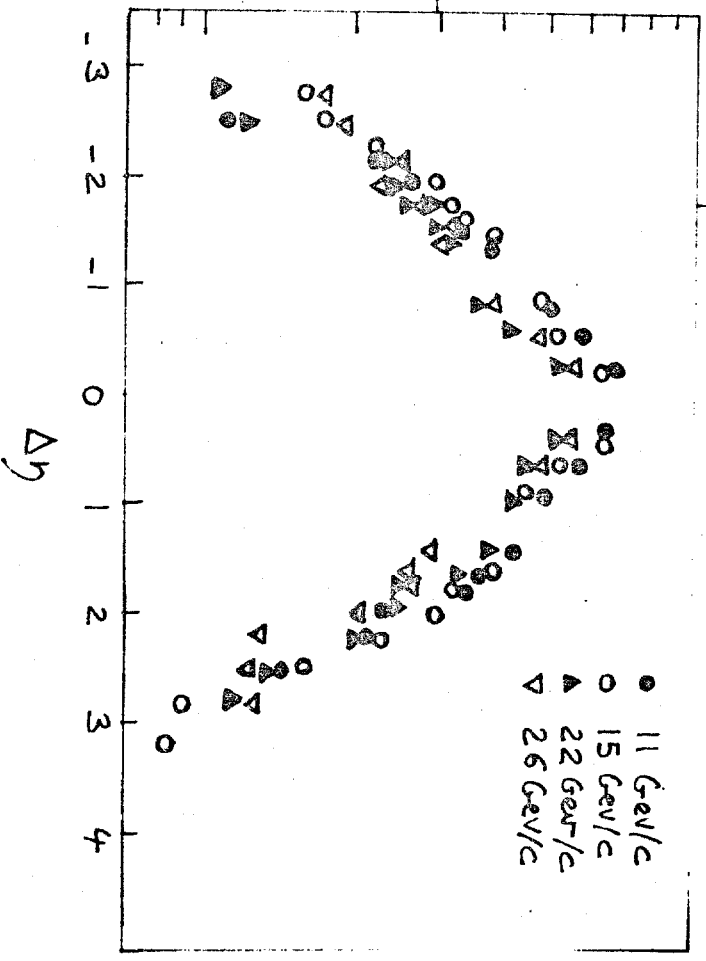


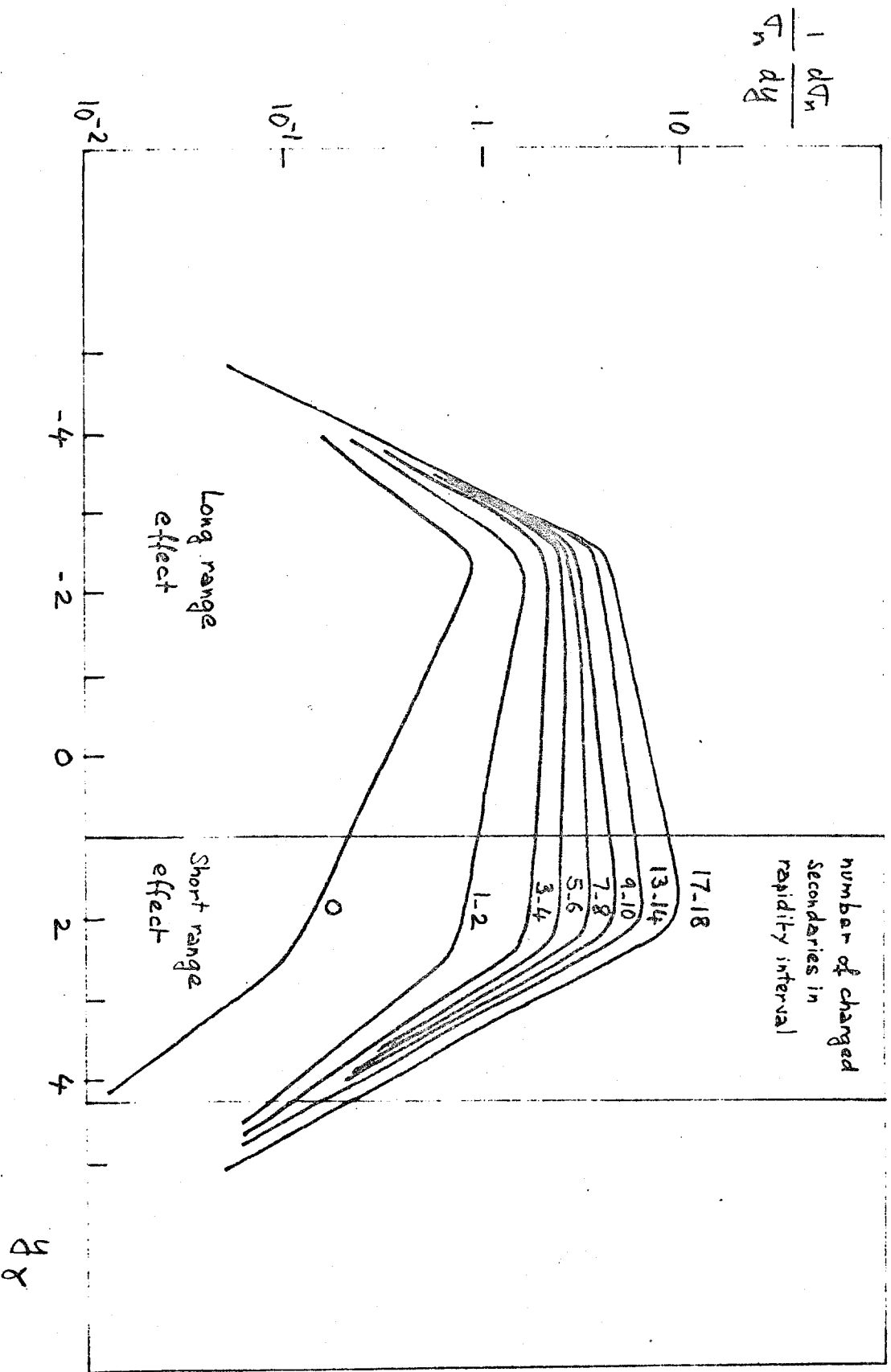
Figure 10-b  
Pisa-Shany Brook

energy dependence



Charged-charged Correlations

figure 11  
CERN-Hamburg-Vienna



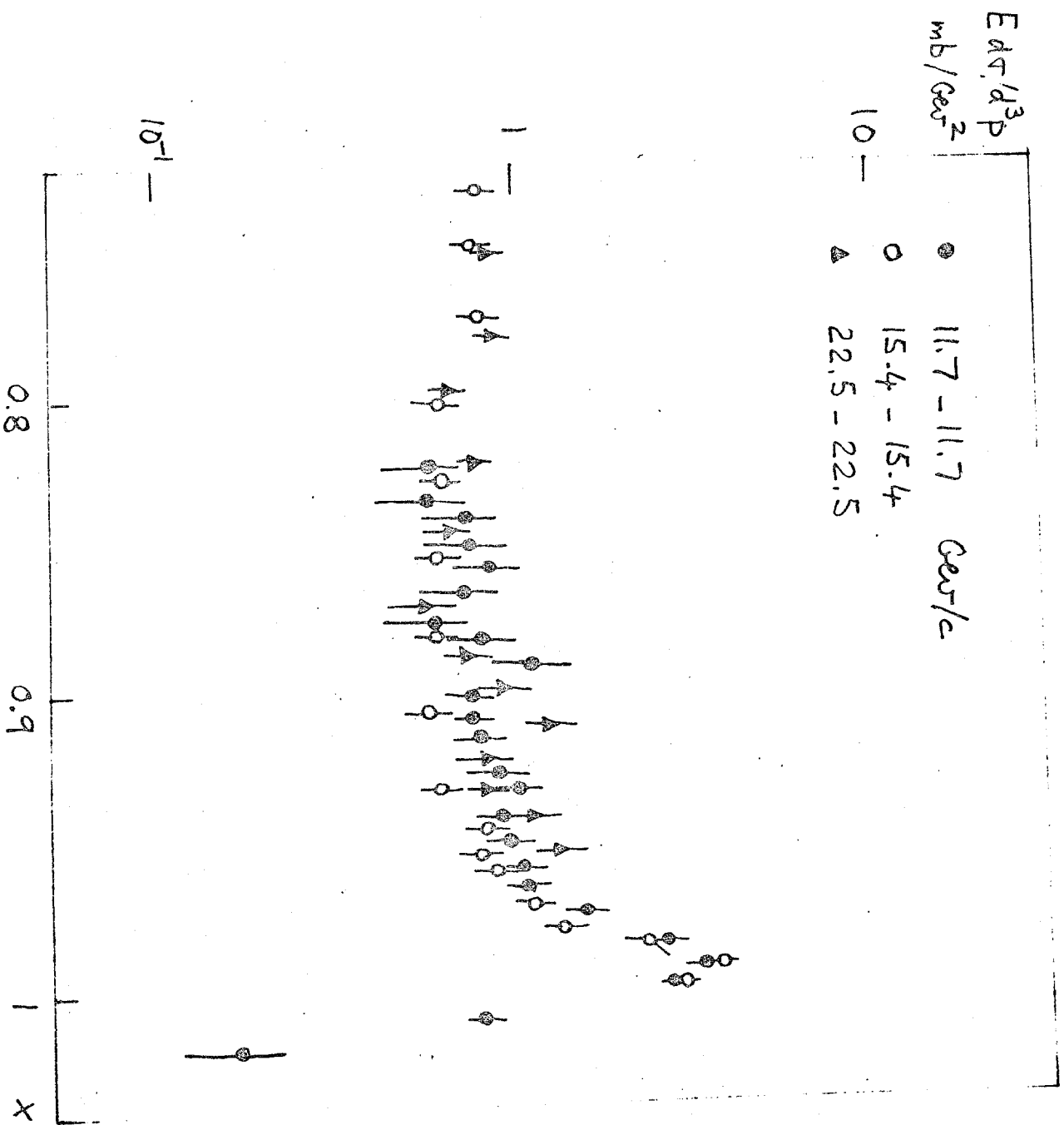


figure 12-a  
 CERN-Holland-Lancaster-Manchester

$PP \rightarrow P + \dots$   
 $P_T = 0.8 \text{ GeV}/c$   
 $1-x \approx s/M^2$

$E \frac{d\sigma}{d^3p}$   
 mb/GeV<sup>2</sup>

10—

1—

10<sup>-1</sup>—

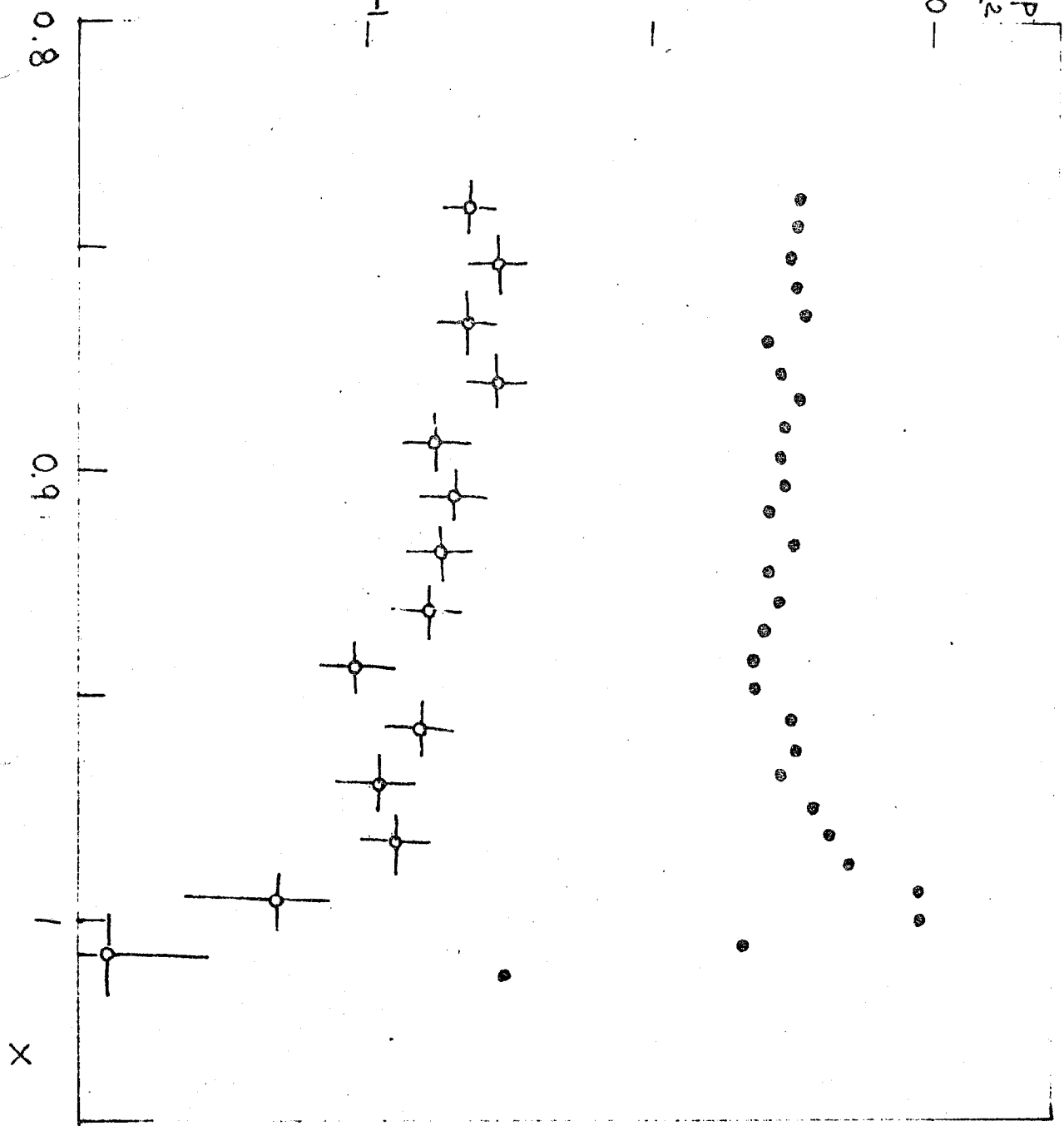


figure 12-6

CERN. Holland. Lancaster. Manchester

$\sqrt{s} = 30 \text{ GeV}$

$PP \rightarrow P + \dots$

at  $\theta = 40 \text{ mrad}$

• Inclusive

○ pion rate at  $90 \pm 14^\circ$  in coincidence with leading proton.